GENERALIZING THE GEOMETRICAL FACTOR THEORY

David Kennedy, *QED* Petrophysics LLC

ABSTRACT

Archie developed his model based upon trends observed in formation resistivity factor - porosity and resistivity index-water saturation plots. The trends appear when the data is plotted on log-log graph paper. The trends are apparently straight lines on log-log paper, which means that they are "power laws" of the form $F = 1/\varphi^m$ and $I = 1/S_w^n$ where m and n are observed to distribute themselves around m and $n = 2$. Archie did not attempt to connect his empirical discovery to any physical first principles, nor did he discuss alternative trends that might have fit the data. However, Archie's model filled a void in formation evaluation, and works well. Four decades would pass before researchers began to attempt to connect conductivity in rocks as described by the Archie model to first principles. Since 1980 several attempts to connect the Archie model to first principles were, and continue to be, made. There has been no generally accepted success in the attempts. Waxman and Smits (following M. R. J. Wyllie, 1952) changed the focus of attention from resistivity to conductivity in 1968. This was a step in the right direction, but they retained Archie's model reformulated in conductivity terms; in that sense there was no change in thinking. The first rethinking of the problem appeared in 1993 by positing three first principles: bulk rock conductivity is proportional to (1) brine conductivity; (2) fractional volume of brine in the rock; (3) a geometrical factor. Brine conductivity and fractional volume of brine (i.e., porosity) are directly measurable, and the geometrical factor can be estimated from measurable quantities. From these "first principles" a model relating bulk rock conductivity to water saturation can be derived. The model, called the geometrical factor theory (GFT), is different from the Archie model, but the Archie model is contained within it as a limiting case. In 2007 a different model based upon a different formulation of the first principles, known as a pseudo-percolation threshold theory (PPTT), was developed. Although different from the GFT, PPTT also contains the Archie model as a limiting case. Since GFT and PPTT are different, it seems as if one of them must be wrong. However, I show that neither is wrong, but both are special cases of a more general model. Whereas Archie analyzed his data in terms of formation resistivity factor versus porosity and deduced a power law, an alternative analysis in terms of formation conductivity factor would have revealed that Archie's data for both formation factor vs. porosity and resistivity index vs. water saturation is fit, arguably better, by a quadratic function. The quadratic function follows directly from first principles, whereas Archie's power law does not. I call the new model the Generalized GFT (GGFT), and show that it subsumes the GFT, PPTT, and Archie's model as special cases. Interestingly, the shaly sand models can also be accommodated in GGFT. As an explanation of the Archie model from first principles has long been a Holy Grail of petrophysics, this is of significant interest.

INTRODUCTION

Genesis. This article will summarize the evolution of thought on the use of resistivity instrument responses to infer hydrocarbon volumes in conventional petroleum reservoirs. To date, such thinking has been happening for over nine decades. Perhaps it is now possible to view past efforts from present knowledge and construct a frame of reference where the most popular methods can be placed and examined in relation to other proposed methods.

As is well known among practitioners of the formation evaluationist's craft, the instrumentation for estimating formation resistivity was introduced by the Schlumberger brothers' company in 1927, (Schlumberger, 1982) and has been undergoing periodic improvements since that time.

Although it was apparent from the very first that high resistivity was correlated with hydrocarbon-bearing formations, that was a "necessary – but not sufficient" condition for the presence of hydrocarbons in a formation. High resistivity could also result from low porosity (and we have since learned that high resistivity is also not a necessary condition – but low resistivity pay was unknown to the pioneers).

More than a decade would pass following the invention of well logging before a model for estimating hydrocarbon volumes from formation resistivity would be developed. This model was derived by empirical observation and graphical analysis of laboratory data, but its purpose was the interpretation of well log resistivity data. The model's inventor, G. E. Archie, offered no derivation of his model from any underlying physical principles, nor even an analysis of possible models that might have been fitted to the observations. It was enough that Archie's model proved efficacious in many (with some exceptions) situations. Indeed, the Archie model was so successful – and quickly became so ubiquitous – that it acquired the honorific "Archie's 'Law' ".

Usually, to gain the status of a "law", a model must follow directly from established, or newly discovered, "first principles". However, the Archie model attracted no interest from academically-minded scholars for many years, and no attempts were made to derive the model from fundamental principles. Consequently, Archie's model remained immune from scrutiny and criticism for a long time. Some effort (notably by M. R. J. Wyllie and coauthors) was devoted to this problem by oil company research laboratories in the decade following World War II (e.g., Wyllie and Rose, 1950; Winsauer et al., 1952). Although the best characterization of this research is that it was inconclusive, at the time it apparently satisfied the curiosity of users of resistivity methods for hydrocarbon volume estimation.

Forty years would pass following the introduction of Archie's model before attempts were made to connect the Archie model to first principles. Sen (1980) published an article with a section titled "Archie's Law from First Principles". The "first principle" that Sen[1] offers is the effective medium approximation (a mixing rule) developed by Bruggeman (1935) and Hanai (1968). To claim "first principle" status for a mixing rule is a misuse, if not abuse, of language. The Bruggeman-Hanai formula in the limit of low frequency reduces to a power law dependence of normalized conductivity to porosity. The power, however, is 3/2 rather than the $4/2 \approx 2$ of the Archie model. Sen claims that this is one of "two derivations of Archie's law from first principles that exist in the literature". However, his citation for the second source in the literature is a personal communication from Prof. Theodore Madden at MIT; it is not "in the

literature". Madden (1976) had published an article in *Geophysics* with a section titled "Archie's law and conduction in porous media". Madden finds for a "simple crack width distribution function" that conductivity is approximately proportional to porosity squared. Madden remarks "… the universality of Archie's law appears to be more an accident of the trends of crack and pore width distribution functions than a fundamental property of porous media." Thus, I suggest Sen's claim is exaggerated. However, I would agree that as of the date of his publication that there were *no* published attempts to derive Archie's model from first principles. Sen rightly deserves the credit for opening the topic for investigation and discussion.

To my knowledge the first attempt to derive the Archie model in a straightforward derivation from first principles is from Herrick and Kennedy (1993, 1994). The principles are three, and simply stated:

The bulk conductivity of an oil-bearing reservoir rock is *proportional* to:

(1) brine conductivity;

(2) fractional volume of brine in the rock;

(3) the geometrical configuration of the brine.

Herrick and Kennedy called this model a geometrical factor theory (GFT) model, based upon the brine in the rock. It applies to the restricted class of rocks (now called "Archie rocks") for which brine is the only conducting phase, and several other conditions (see Appendix A). However, these rocks were primary targets for petroleum exploration for more than a century.

A further attempt to discover a principle by examination of experimental data is found in my article (Kennedy, 2007). The model is called the pseudo-percolation threshold theory (PPTT), to be summarized later.

The GFT and PPTT models are not the same except in the limit of a vanishing percolation threshold, in which case both models reduce to the Archie model. One's first instinct is to conclude that since they are not the same, either GFT or PPTT must be wrong; however, an alternative that unifies them is that both are special cases of a more general model. The more general model thus subsumes models derived from first principles such as GFT and from observation such as PPTT and the Archie model. This article will

---

[1] Without attribution to Bruggeman or Hanai.

introduce a generalization of the geometrical factor theory (abbreviated as GGFT).

Since the GGFT will bring together as special cases all of GFT, PPTT, and the Archie model, it seems appropriate to provide the historical context of the development of these models. Thus, I shall begin with a recounting the foundations of Archie's model as cited, but not discussed, by Archie himself.

HISTORY

The Need for a Method. Well logging, first demonstrated in 1927, had become a ubiquitous tool in the evaluation of oil wells a decade later. It was qualitatively useful for differentiating hydrocarbon-bearing from brine-bearing formations, but there was no means to convert an apparent resistivity into an estimate of hydrocarbon in place. This changed with Archie's announcement of his model to the world in 1941 at the Dallas meeting of the Petroleum Division of the AIME and its subsequent publication in 1942. Archie's understated title is: *The electrical resistivity log as an aid in determining some reservoir characteristics*. A more descriptive title might have been: *The electrical resistivity log as the key in determining reservoir hydrocarbon volumes.* That is certainly what Archie's technique became almost immediately thereafter.

Archie's Model. Archie developed his model based upon porosity-resistivity data that he collected in Texas and Louisiana oil fields, and water-saturation – resistivity index data from four references in the late 1930s literature. His model is based upon trends that he noticed when he plotted this data on log-log graph paper. These trends were condensed into six equations culminating in the model that has become known in the oilfield vernacular as Archie's "law". Archie knew from his own research that the ratio of bulk rock resistivity to brine resistivity for a given core is constant; i.e., $R_0/R_w = F$, which he called the formation resistivity factor, and which he introduced as $R_0 = F R_w$. Plotting the formation resistivity factor against porosity on log-log graph paper, the trend that emerges suggests a straight line. A straight line on a log-log grid translates into a power law which Archie expressed as $F = \varphi^{-m}$, or $R_0 = R_w \varphi^{-m}$. The data that Archie cites in the literature is presented in three forms. Archie, in a stroke of genius, realized that all of the data could be converted into water saturation and resistivity index (although that term had not yet been coined) and plotted as resistivity index (i.e., $I = R_t /R_0$) versus water saturation on log-log paper.

The trend suggested by this data was also a power law which Archie expressed as $I = R_t /R_0 = S_w^{-n}$, or $R_t = IR_0$. Substitution of the trend for R_0 into this relationship gives $R_t = R_w \varphi^{-m} S_w^{-n}$. This is what has become known as the Archie law. Interestingly, Archie himself did not offer this form of his relationship, but expressed it directly in terms of S_w; i.e., $S_w = (FR_w/R_t)^{1/2}$ (Archie, 1942, eqn. 6).

In essence, Archie's law is based upon the trends observed in the two plots shown in figures 1 and 2, reproduced from Archie's 1942 article. Archie offered no speculation on how his model might be connected to the physics of conduction in rocks, or whether his dual power law model was unique. His analysis is based upon unabashed empiricism; it has served the industry well for eight decades. As already mentioned, it would not be until the 1980s that industry researchers began to seek a connection of the Archie model to conductivity first principles.

Although in 1941 much progress still lay ahead in porosity and resistivity logging technology, Archie's technique could be usefully employed with then-existing downhole methods of formation resistivity and porosity estimation. Indeed, (as you know) Archie's model, and embellishments thereof, continues as the foundation of much, if not most, interpretation technology to this day.
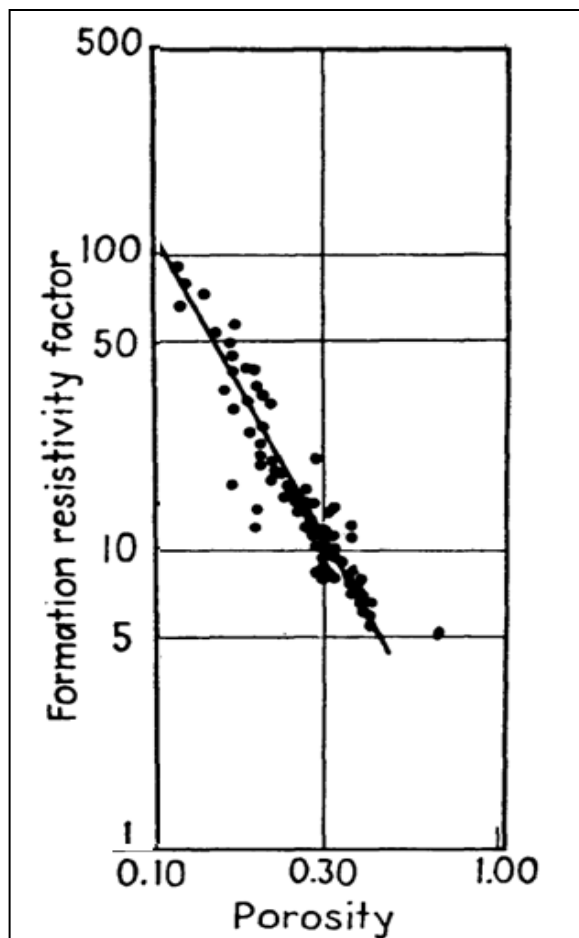
If there is one unfortunate result of the success of Archie's model, it is that it tended to stifle further thinking about the interaction of hydrocarbon, brine, and pore geometry to produce the formation resistivities observed using well logs. This lack of a theory based upon physical principles has tended to separate petrophysics from the mainstream of geophysics, making it a niche discipline. Adoption of a theory grounded in first principles would unite petrophysics with other disciplines of exploration and production geophysics.

FIRST OBSERVATIONS

Imagine yourself in Archie's place in the late 1930s by examining the references that he cites in his 1942 seminal paper.

Archie's model rests upon two kinds of observations, both made on core specimens in laboratories: these are the observation of specimen resistivity index as water saturation is reduced from 100 percent to as low as could be attained with the apparatus in the laboratory (known as a "drainage" experiment), and the observations of formation resistivity factor of a

collection of specimens plotted against porosity. The resistivity index – water saturation data that Archie uses is from four sources in the literature: Wyckoff and Botset (1936); Jakosky and Hopper (1937); Leverett (1938); Martin et al. (1938). These data are presented in three different formats, with only one of the data sets given as a list of numbers and two of the papers mainly concerned with flow through unconsolidated sands rather than specimen resistivity. It is to Archie's great credit that he was able to recognize these data as being fundamentally similar despite their dissimilar-looking representations. The data from these references are reproduced in figures 3 through 6. These data are converted to resistivity in-

dex and plotted as a log-log graph in figure 7 and are the basis for Archie's figure 3.

RESISTIVITY INDEX VS. WATER SATURATION

Wyckoff and Botset - 1936. As part of a study of the flow of gas-liquid mixtures through unconsolidated sands, Wyckoff and Botset used conductivity in their apparatus in order to estimate the volume of gas present in their flow experiment. The data they published is basically the calibration for their apparatus. Their specimens were one sample of Berea sandstone at 19.95 percent porosity and three sand packs engineered to have porosities of 27.78, 35.4, and 42.96 percent porosities. They presented their results graphically as water saturation versus conductivity index.

Their figure is reproduced here as figure 3. Interestingly, all these data fall along a single trend regardless of their differing porosities. The points plotted are not distinguished by porosity, but are visible enough to digitize. This has been done and the data will be used and discussed later.

Jakosky and Hopper - 1937. Jakosky and Hopper reported on their research in the article *The effect of moisture on the direct current resistivities of oil sands and rocks*. By "moisture" they are referring to water saturation. This was exactly what Archie was interested in, so the paper appeared to be perfect for his studies, and provided a table of data in addition to plots. However, their method introduced uncertainty

Figure 1. The seminal data set for Archie's model is the Nacatoch sandstone. The graph shown here was Archie's figure 2. The data are from Bellevue field, northeast of Shreveport Louisiana. The formation at that location is about 3000 feet in depth. The original figure is postage-stamp sized, but most of the points can be individually resolved.
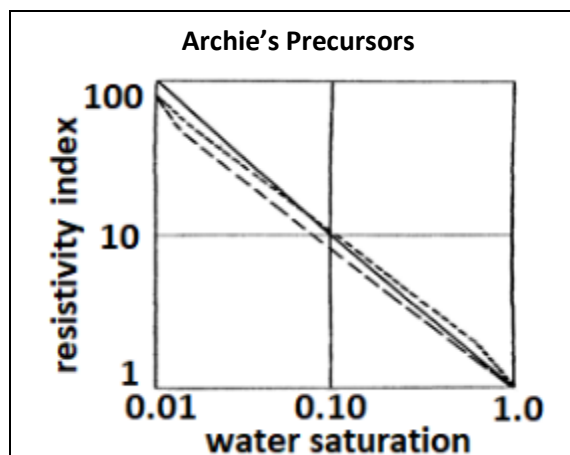

Figure 2. Archie's resistivity index versus porosity data, as shown in his figure 3. Archie plots the data in power-law format, however this is not the only way to represent the functional form of the data. Archie's horizontal and vertical axes have been exchanged to conform to the modern plotting convention.
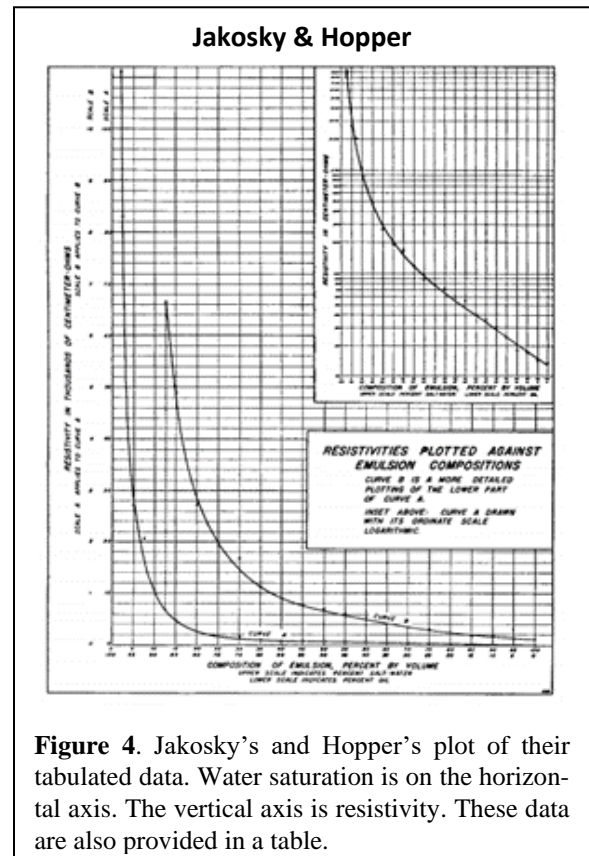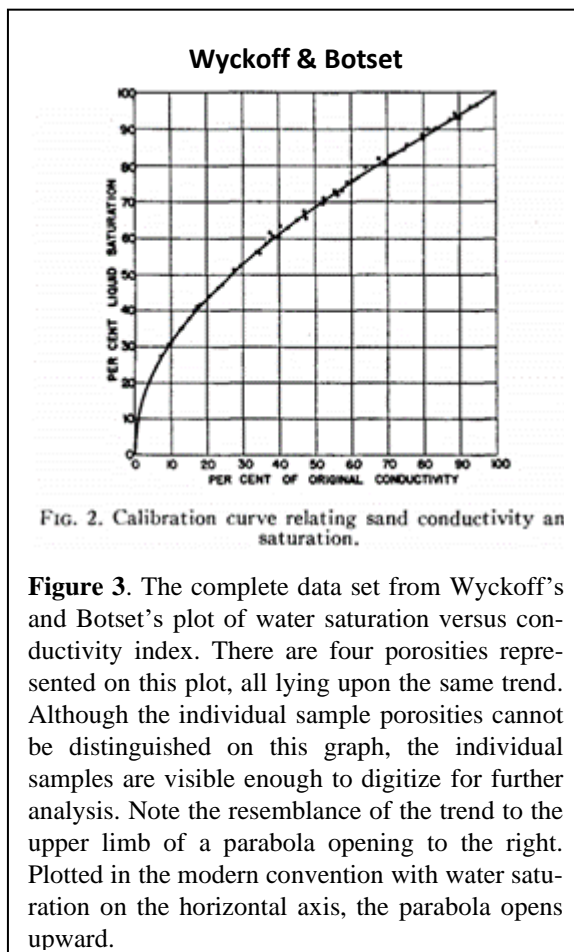
in their results, unquantified in their paper.

Their 24 specimens, collected on a road cut outcrop about a mile north of the UCLA campus, were assumed to have the same porosity as an average of the first two specimens measured, which differed by 1.65 porosity units. They used the average of these two, 23.2 percent, as an estimate of porosity for all of their samples. This lack of porosity control undoubtedly contributed to the scatter observed in their data. However, insofar as the average porosity was representative, it was a mid-range porosity in a consolidated rock, useful for corroboration of Archie's hypothesis regarding the trend in the resistivity index – water saturation data. Their plot is reproduced in figure 4.

The data for this plot was obtained using an unconventional procedure. Instead of the usual practice of desaturating a single specimen saturated with the wetting phase fluid (i.e., brine) and noting its decrease in conductivity (i.e., drainage), they chose 24 specimens (implicitly deemed to be identical in po-

rosity and pore geometry) and infused each specimen with one of 24 oil-brine emulsions of brine content differing by 5 percent increments, except at the lowest water saturations where the increment was 2.5 percent. Note that this method is neither imbibition nor drainage. Although the specimens were carefully cleaned and dried before the emulsions were infused, there would have been no way to ascertain and confirm whether the emulsion would have separated into two continuous, interpenetrating phases with the brine wetting the mineral grain surface and the oil occupying the central region of the porespace in their specimens.
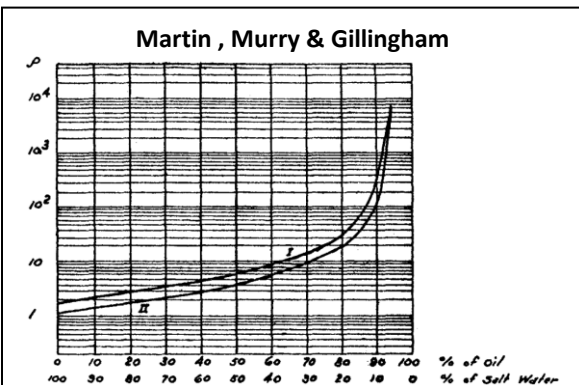
Although pore geometry is not mentioned in the paper, the specimens are implicitly assumed to have the same pore geometry (indeed, they are implicitly assumed to be the same core to simulate a drainage experiment); otherwise, it would make little sense to order them in a progression of increasing water saturation. However, due to the lack of control on porosity (probably different for each specimen), pore geometry (also probably different for each specimen), and on the brine wettedness of the grains, this dataset is problematic. Among the four data sets that Archie incorporated as inspiration for, and the construction

Wyckoff & Botset

FIG. 2. Calibration curve relating sand conductivity an saturation.

Figure 3. The complete data set from Wyckoff's and Botset's plot of water saturation versus conductivity index. There are four porosities represented on this plot, all lying upon the same trend. Although the individual sample porosities cannot be distinguished on this graph, the individual samples are visible enough to digitize for further analysis. Note the resemblance of the trend to the upper limb of a parabola opening to the right. Plotted in the modern convention with water saturation on the horizontal axis, the parabola opens upward.

Jakosky & Hopper

RESISTIVITIES PLOTTED AGAINST EMULSION COMPOSITIONS

Figure 4. Jakosky's and Hopper's plot of their tabulated data. Water saturation is on the horizontal axis. The vertical axis is resistivity. These data are also provided in a table.

of, his model, this one is the most "scatter prone". The curves fitted to the points in figure 4 must have been drawn "by eye" using a French curve, as digitized versions of these curves are not well-fit by either power-law or quadratic functions in Excel's trendline tool-kit (see figure 10).

Martin, Murray, Gillingham - 1938. Martin, Murray, and Gillingham provide two resistivity curves plotted against water saturation. There are no data points on their chart, nor in their paper. The two curves are for porosities of 0.20 and 0.45 respectively and are representative of "a great number of experiments". Their plot is reproduced in figure 5. The brine resistivity is given as a "solution of NaCl of 12° Baumé." The standard temperature for measuring degrees Baumé is 16° C (60° F). MM&G are silent regarding the temperature during their measurements. Assuming 16° C as the temperature, the density of the brine was 1.09 g/cm^3, or about 170,000 ppm NaCl. At the standard temperature (i.e., 60 ° F), this corresponds to a resistivity of about 0.07 ohm-m.

Archie converted these curves to resistivity index by dividing by R_0, the resistivity at 100 percent S_w. In practice he probably traced the curves on compatible semi-log graph paper, and then slipped the point at $S_w = 1$ down to a resistivity of 1; then he could read resistivity index directly from the slipped graph paper[2] Note that there are two slope trends exhibited by each curve with the slope approximately constant for

higher brine saturation, and again approximately constant but with much higher tilt at lower brine saturation. MM&G do not remark upon this.

Archie uses only the trend for $S_w > 0.10$ in support of his model[3] and makes no mention of the second trend for $S_w < 0.10$.

It is interesting to note that as part of the discussion of this figure MM&G remark: "The conductivity of a sand … will depend upon its porosity, and it will be proportional to the conductivity of the adsorbed water …". In this sentence they have briefly switched the focus of their thinking from resistivity to conductivity, and they have identified two of the three principles that will form a part of the geometrical factor theory. They omit only the role of brine geometry from their thought. They then immediately switch back to discussing resistivity since that is what they measured directly on the core specimens that they used. Had they given more thought to the problem in conductivity terms, they might well have anticipated the GFT by 55 years, and preceded the Archie model by 4 years. It is a lesson regarding building a box for one's thinking too soon, for it will become very hard to think outside of it once built.

Figure 6. The complete data set from Leverett plot of water saturation versus conductivity index. Note the similarity to Wyckoff and Botset.
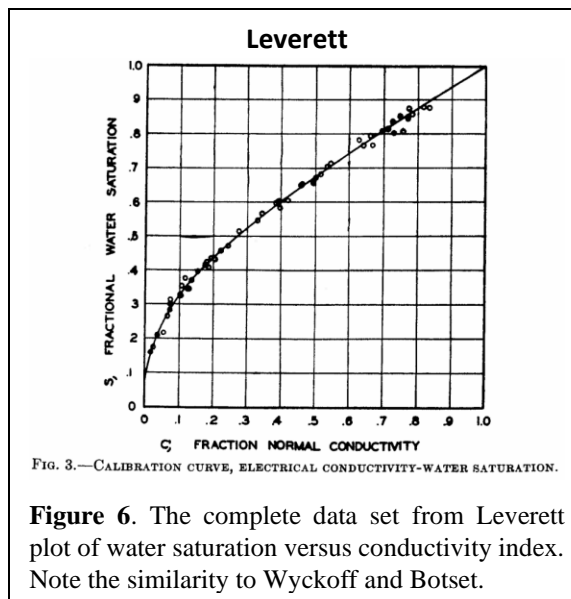

Figure 5. The resistivity data of Martin et al. There are no data points on the chart. Note the shape of curve is basically similar to that plotted by Jakosky and Hopper except for the reversal of the water saturation axis, and extension of the resistivity axis an additional decade upward.

[2] This method was well-known to users of slide-rules in pre-hand-held calculator days.

[3] The MMG datasets show two trends, one for porosity less than 10 percent, and another for porosity greater than 10 percent. Archie used only the second trend in his analysis. Following Archie's lead, this analysis uses the data greater than 10 percent. The break in slope is probably due to the disconnecting of the brine phase as brine saturation is lowered below 10 percent.
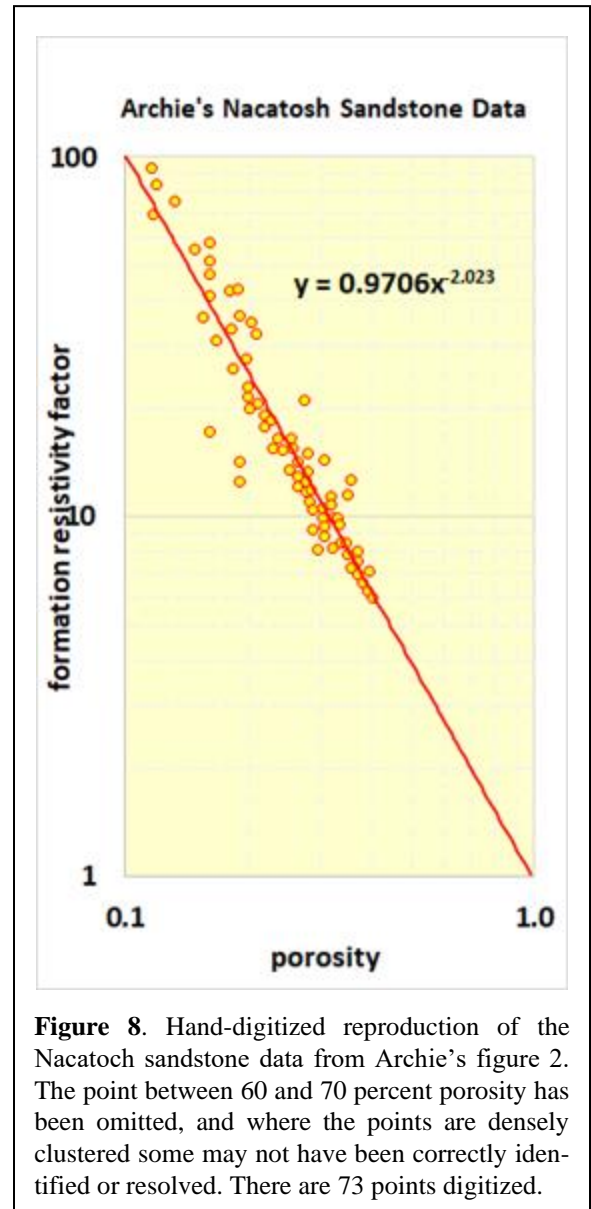
Leverett - 1938. Leverett essentially repeated the experiment of Wycoff and Botset. He used four sandpacks as specimens with porosities of 0.41, 0.42, 0.40, and 0.41. Except for the data points, Leverett's plot is essentially identical to the plot of Wyckoff and Botset; it is included here as figure 6.

Summary. Plotting the observations reported in these four precursor publications provided Archie with a trend applicable to many clastic and some carbonate rocks. The trend has a particularly simple expression as a power law, and is a straight line on log-log graph paper. The precursor data sets are shown with Archie's representations of the trends that he observed in figure 7.

As an aside I observe that one puzzling aspect of these data is that the slope of the power-law trend is uniformly close to $n = 2$, whether from sandpacks or from specimens from rocks. This is in contrast to formation resistivity factors determined from sandpacks which tend to be much lower than those observed on sandstones from quarries. Archie cites $m = 1.3$ as typical for sand packs. This difference between m and n in sandpacks is, as I note above, puzzling.
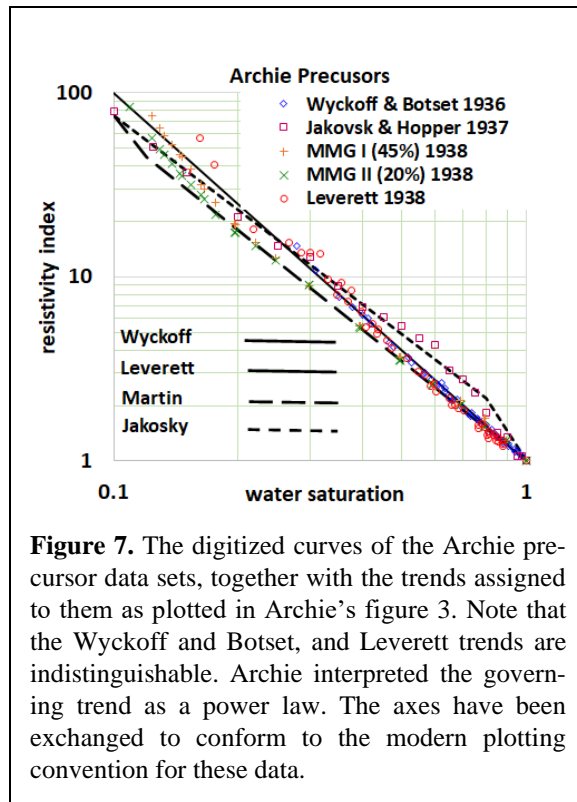
Archie's Observations. Archie's own contribution to his data is a list of formation resistivity factor versus porosity, which he presented as postage-stamp-sized scatter plots. In Archie's figure 1 he composites data from seven fields (Southeast Premont, Tom Graham, Big Dome-Hardin, Magnet-Withers, Sheridan in Texas and La Pice and Happytown in Louisiana). The porosity range of these data is from somewhat less than 0.20 to somewhat more than 0.30. It is true that it forms a "cloud" with a trend, however it is not clear what conclusion can be drawn from this. There is no specification of the producing formations and other meta-data (such as formation age) that might help in defining trends. Perhaps we could sur-

Figure 7. The digitized curves of the Archie precursor data sets, together with the trends assigned to them as plotted in Archie's figure 3. Note that the Wyckoff and Botset, and Leverett trends are indistinguishable. Archie interpreted the governing trend as a power law. The axes have been exchanged to conform to the modern plotting convention for these data.

Figure 8. Hand-digitized reproduction of the Nacatoch sandstone data from Archie's figure 2. The point between 60 and 70 percent porosity has been omitted, and where the points are densely clustered some may not have been correctly identified or resolved. There are 73 points digitized.

mise that the behavior of all of these (and by implication, all other) "Gulf Coast Sandstones" is similar regardless of formation. (this is – arguably – approximately true). Figure 1 (Archie's figure 2) is for a single formation in a single field, the Nacatoch sandstone in the Bellevue field Louisiana. The porosity range is large: 0.10-to-0.40 porosity units. Archie does not describe the formation in his 1942 paper. In a later paper (Archie, 1950) he describes the Nacatoch sandstone as "Friable sandstone, poorly sorted grains, shaly and calcareous; comparatively high porosity for permeability." This data set is remarkable, and just what Archie needed to illustrate his model, in that (after removing some obvious outliers) it is very nearly a perfect candidate for a power-law fit of the data with porosity raised to the second power (−2.023) and coefficient one (0.9706), and the trend passing almost exactly through the brine point ($\varphi = 1$, $F = 1$) and origin ($\varphi = 0$, $1/F = 0$). The power-law coefficient and exponent as determined by Excel's trendline tool are displayed on the chart in figure 8.
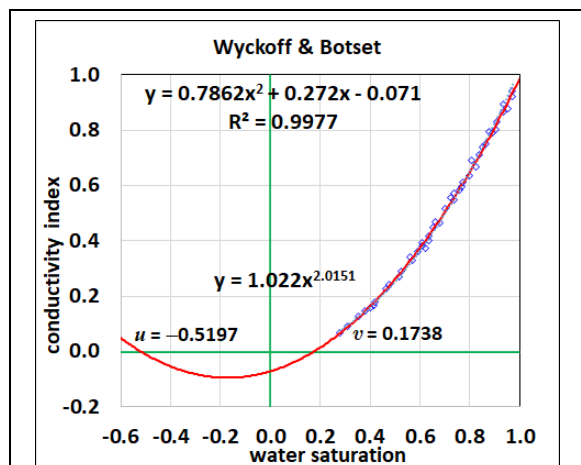
FIRST OBSERVATIONS REVISITED

Review. As just discussed, Archie's model followed from observations of conductivity and resistivity of various natural and synthetic rocks as brine saturation was varied from fully brine saturated down to irreducible brine saturation. Archie noticed that when the various data were expressed as resistivity index and plotted against water saturation, or formation resistiv-

ity factor versus porosity, the trends that he observed were well-represented by power laws, or a straight lines when the data is plotted on log-log graph paper. He also showed the connection between the two power laws (R_0 appears in both and could, thus, be eliminated from one) to produce the first porosity – resistivity – water-saturation model.
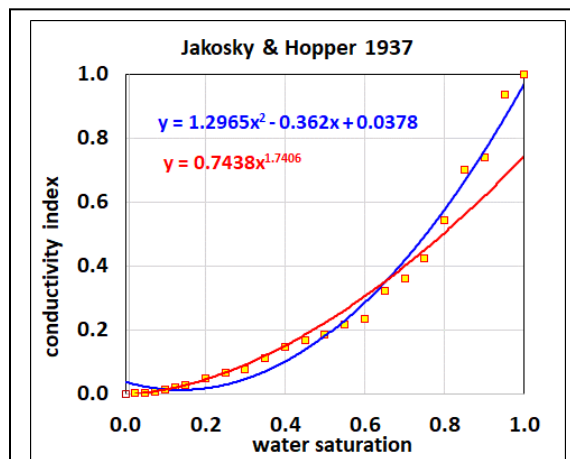
Since Archie published his data only as postage-stamp sized plots, this would have made further analysis of the data in other formats quite difficult in the pre-electronic computer era.

Archie's model (as published) was so immediately useful that it seems not to have occurred to contemporaneous researchers to consider alternatives. I illustrate plots of these seminal data sets represented as conductivity index versus water saturation, and formation conductivity factor versus porosity in figures 9 through 17.

Reconsidering the Seminal Observations. It is fitting to be able to use the same data as the pioneers of petrophysics to illustrate they could have built different models from their data. It is also unfortunate that oil companies are stingy with their published data;

Figure 10. Jakosky's and Hopper's data fitted using Excel's built-in trendline tool. The quadratic fit (blue curve) does a fair job at high water saturations, but does not match other points well and has no real roots (that is zeros); the power law fits only at low water saturations. Given that this plot is not a true resistivity versus water saturation plot taken on a single specimen, the departure from the well-defined trend that is usually observed is not surprising. This data is the least well-behaved and least corroborative of Archie's hypothesized power-law fit of the trend.

Figure 9. Resistivity index versus water saturation data from Wyckoff and Botset, presented as conductivity index versus water saturation on linear scales. The roots of the quadratic in this case are $u = -0.5197$ and $v = 0.1738$.

and thus these seminal publications spanning, now, eight decades remain among the most readily accessible data for studies such as this one.

CONDUCTIVITY INDEX - WATER SATURATION

Conductivity Index vs. Water Saturation. Archie's data was recorded in terms of resistivity, whether in reports of special core analysis from laboratories, or apparent resistivities from well logs. It is natural that he would formulate his model in terms of resistivity.
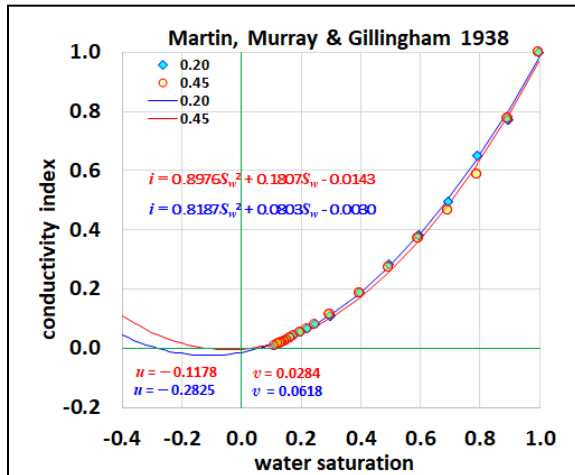
However, it is informative to look at this same data from a different perspective. In terms of electrical properties of materials, the alternative choice is conductivity.

For Archie's four resistivity-index – water-saturation data sets, the curves are all parabolic in shape, and except for the noisy data of Jakosky and Hopper, are fit by quadratic functions with high fidelity. Figure 13 combines the data of Wyckoff and Botset with those of Leverett and are fit by a single quadratic.

The point is that all of these data are very suggestive that the underlying function is a quadratic polynomial. The "standard" form for a quadratic equation expressing conductivity index as a function of water saturation is

$$i = a_i S_w^2 + b_i S_w + c_i \qquad (1)$$

where $i = \sigma_t / \sigma_0 = 1/I$ is normalized specimen conductivity, or conductivity index, and a_i, b_i, and c_i are

constants, and I is resistivity index.

Looking now at the Nacatoch sandstone data set in terms of conductivity, figure 14 reproduces the entire data set as normalized conductivity versus porosity. At the scale of figure 14, a linear trend would make adequate predictions of normalized conductivity given porosity. However, if the fitting function is required to contain the brine point, a straight line will not meet the requirement. A quadratic polynomial does accomplish the job of fitting the observations and including the brine point[4] (figure 15). The quadratic has the standard form

$$f = a_f \varphi^2 + b_f \varphi + c_f . \qquad (2)$$

Fitted with the coefficients from the Nacatoch Sandstone data set, this becomes

$$f = 0.99812\varphi^2 + 0.000479\varphi - 0.000395$$

where the three outliers northwest of the main trend are omitted from the fit, and the brine point is included. The coefficient of determination is $R^2 = 0.9884$. (The corresponding power law fit using all the data and omitting the brine point is $f = 0.9706\varphi^{2.0228}$, with $R^2 = 0.8867$, showing that the Nacatoch sandstone is close to that limiting case for the quadratic which is a power law; i.e., $f \approx \varphi^2$.) Figure 16 zooms the view
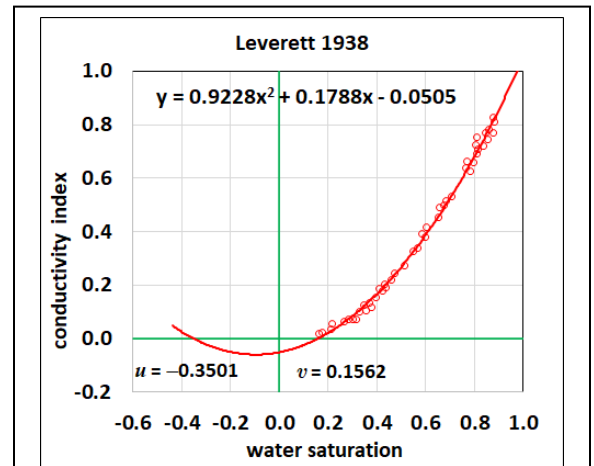
Figure 12. Resistivity index versus water saturation data from Leverett, presented as conductivity index versus water saturation on linear scales. The roots of the quadratic in this case are $u = -0.3501$ and $v = 0.1562$.


Figure 11. The complete data set from Martin, Murray and Gillingham with each of their two curves fit separately by a quadratic function. The zeros of the blue curve are −0.2825 and 0.0618; the zeros of the red curve are −0.1178 and 0.0284.

---

[4] The three points that lie to the "northwest" of the main collection of points are omitted from the fit as they seem to be outliers, more conductive than the other points having similar porosity in the trend. If these points are included in the fit, the resulting polynomial has complex roots.

closer to the origin, and even at this scale it is not apparent that the function has more than a single zero. Figure 17 zooms in even closer, and at the scale of figure 17 it is apparent that the parabola has two zeros. These zeros, located at −0.01965 and 0.02013, are located almost symmetrically about the vertical axis with the normalized conductivity axis intercept at −0.000395, very close to zero. Note that the coefficient of the linear term and the constant are both approximately zero, while the coefficient of the squared term is approximately 1. Thus, the Nacatoch sandstone approximates a power law with coefficient 1 and exponent 2. (You might well wonder if a power law has a representation as a polynomial. Are the two representations equivalent? That question is investigated in Appendix B.)

Archie's Nacatoch Sandstone data set is atypical in its nearness to a power law (i.e., a "standard" quadratic function with $a = 1$, $b = c = 0$). A more typical example of a sandstone trend is provided by the data set published by Winsauer et al. (1952), and illustrated in figure 18.
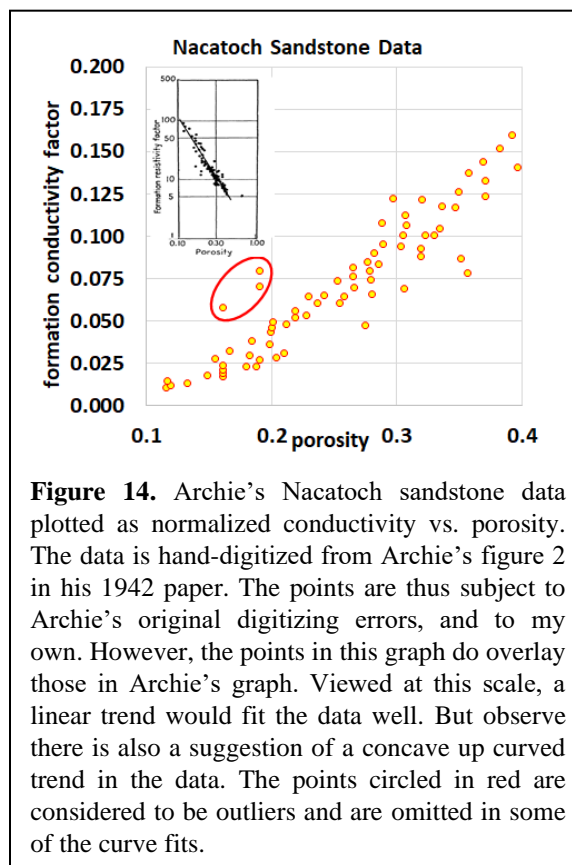
ROCK MODEL

Standard Practice. One of the standard practices in formation evaluation is to plot formation resistivity factor against porosity and describe their correlatability with a trend line and its formula. The trend line is
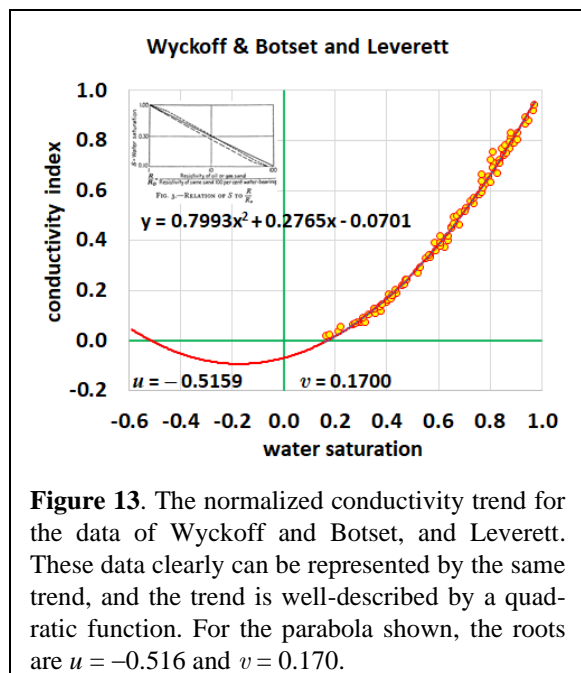
then used to predict resistivity from porosity. Empiricism discourages extrapolating a trend outside the boundaries of the data used to establish the trend to project resistivity to lower or higher porosity, especially if the porosity range in the data is small.

But what are we to think of this trend in variation of resistivity with variation in porosity? By fitting a trend line to the data aren't we implicitly assuming there is some predictable relationship between a change in porosity and a change in conductivity that can be described by a continuous function. For a known brine conductivity, if the bulk-rock model is extrapolated to 100 percent porosity, then the conductivity of the bulk-medium at that point (i.e., the brine point) is also known with absolute certainty. If we extend the model toward lower porosity then it is expected that a bulk-rock conductivity will become zero at some low porosity value. If observations in rocks as well as the two theoretically known points can be tied together with the same trend line, as they often can be, are we not justified in positing a theory that explains the trend and connects the empirical observations with the theoretical end points of the trend?

Figure 14. Archie's Nacatoch sandstone data plotted as normalized conductivity vs. porosity. The data is hand-digitized from Archie's figure 2 in his 1942 paper. The points are thus subject to Archie's original digitizing errors, and to my own. However, the points in this graph do overlay those in Archie's graph. Viewed at this scale, a linear trend would fit the data well. But observe there is also a suggestion of a concave up curved trend in the data. The points circled in red are considered to be outliers and are omitted in some of the curve fits.

Figure 13. The normalized conductivity trend for the data of Wyckoff and Botset, and Leverett. These data clearly can be represented by the same trend, and the trend is well-described by a quadratic function. For the parabola shown, the roots are $u = −0.516$ and $v = 0.170$.

Thought Experiment. Sandstones originate in a number of ways. A laboratory experiment to model the subaqueous deposition of a sandstone imagines a continually stirred beaker of brine, together with an apparatus for dynamically measuring the conductivity of its contents. As the brine is stirred, quartz grains are systematically added (and an equal volume of brine removed) to the beaker and its conductivity recorded as a function of fractional brine volume. The slurry in the beaker eventually reaches a quartz

fraction where all the quartz grains are in contact with other quartz grains, with the conductive brine occupying the inter-grain void space; i.e., the porosity. The porosity can be further reduced by shaking the beaker and compressing the sand by putting a loaded piston on the top of sand in the beaker. Eventually this results in a minimum porosity. At this
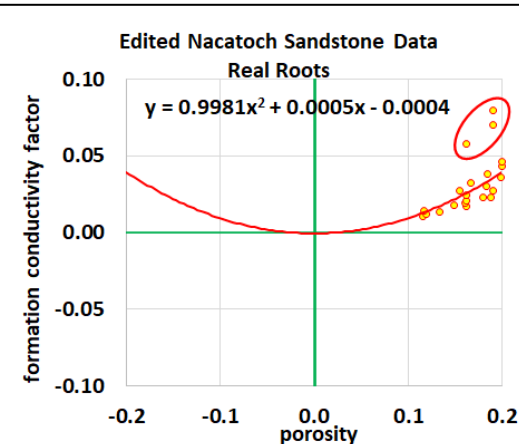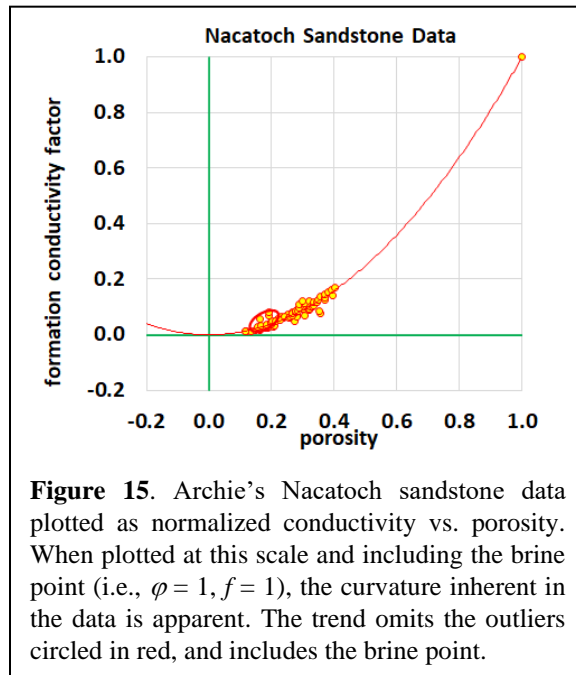
Figure 15. Archie's Nacatoch sandstone data plotted as normalized conductivity vs. porosity. When plotted at this scale and including the brine point (i.e., $\varphi = 1$, $f = 1$), the curvature inherent in the data is apparent. The trend omits the outliers circled in red, and includes the brine point.

Figure 16. The Nacatoch sandstone data set with second-degree polynomial trendline fitted by Microsoft Excel illustrating that the trend suggested by the data passes almost exactly through the origin. The points circled in red are considered to be outliers and are not included in the fit.
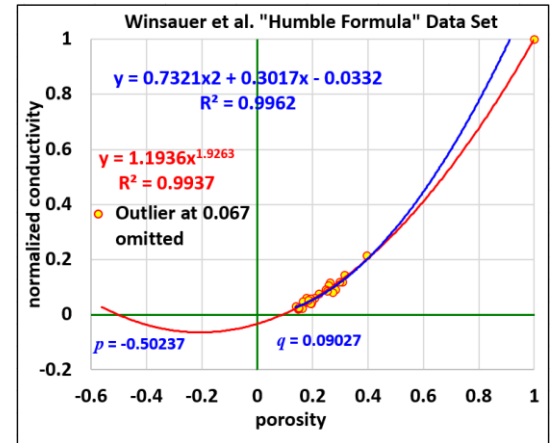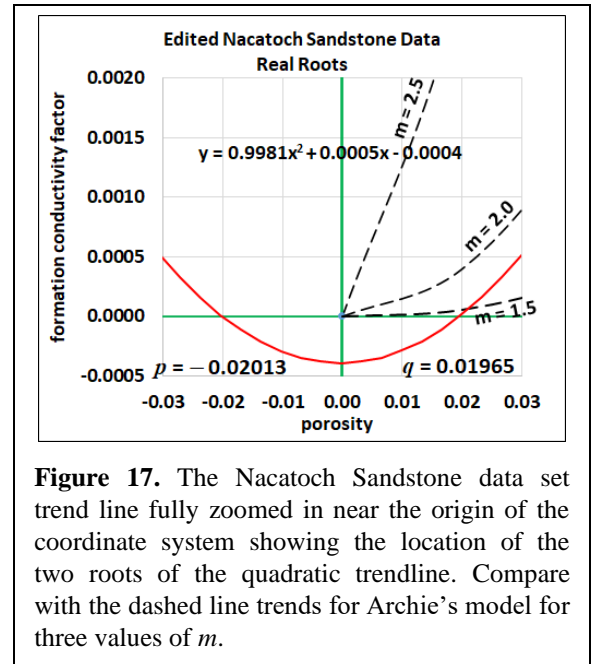
Figure 17. The Nacatoch Sandstone data set trend line fully zoomed in near the origin of the coordinate system showing the location of the two roots of the quadratic trendline. Compare with the dashed line trends for Archie's model for three values of m.

Figure 18. Winsauer's (et al.) data set, with brine point added, and a quadratic trend function fitted to the data. The zeros of the trend line are 0.0903 and −0.5024. The zero at $\varphi = 0.0903$ is the quasi-physical pseudo-percolation threshold. The power law trend line is also fitted to the data omitting the brine point. The power law fit would intercept porosity = 1.0 at a (non-physical) formation conductivity factor of 1.4838 (= 1/0.67 $\approx$ 1 / 0.62).

point the porosity is imagined to be further reduced by inducing cementation of the grain-pack, and even further reduced by grain dissolution and recrystallization. This final mechanism would require the addition of heat and an increase in pressure; i.e., the onset of advanced diagenesis.

The conductivity of this model rock is a continuous function of porosity. At 100 percent porosity, the bulk conductivity is the same as the brine conductivity. Any accurate model function of conductivity versus porosity $\sigma(\varphi)$ must contain this brine point. The conductivity must finally vanish at some low porosity value, not necessarily zero, since the conducting brine film on the grains is eventually obstructed or ruptured and pore throats occluded as the grain phase increases in fractional volume.

The final result of the experiment would be a list of fractional brine volume and conductivity at each stage in the experiment. The experiment is performed under controlled conditions, but the process is similar to the "evolution of a sedimentary rock" in the wild, imagined to proceed from 100 percent porosity (say just above the suspended load in a flowing stream) through the sedimentation phase of deposition with the "liquid-supported" slurry decreasing from 100 down to about 48 percent where the mixture of brine and solids begins to become grain supported, followed by compaction, cementation, and chemical diagenesis removing porosity until it is almost entirely removed, leaving only disconnected isolated porespace. Of course, few real rocks would complete this entire evolution. But, when postulating a relationship between bulk rock conductivity and porosity, this provides an implicit justification in the search for a trend.

It is obvious that conductivity is a continuous function of porosity. It is not so obvious that it should be smooth and without cusps. For example, at the point in deposition where the medium transitions to being grain supported, the rate of change in conductivity with change in porosity (i.e., the slope of the function) might change discontinuously; likewise, at low porosity where pore throats begin to occlude and brine films rupture, there would be another change in slope. Since these cusps, when and if they exist for particular data sets, would be unobservable, there is no choice except to ignore the possibility that they exist. Some data sets will not succumb to efforts to fit them with the model presented here. The existence of the postulated cusps would be a possible explanation.

For data that resist being fit by the trends available in this model, other models must be used.

In the words to follow, I will, working from "first principles", boundary conditions, and the observations of our pioneers, construct a continuous and smooth conductivity model. The model is not a rock; however, it can be used to predict the behavior of rocks over the range of porosities encountered in conventional petroleum reservoirs.

FIRST PRINCIPLES

The Postulates. I introduced David Herrick's first principles in the preamble to this article. I now expand upon those remarks.

According to Wikipedia, "A first principle is a basic proposition or assumption that cannot be deduced from any other proposition or assumption". To my knowledge the first person to devote any thought to first principles for conductivity in rocks was David C. Herrick[5]. His first principles were debuted in our 1993 SPWLA *Transactions* article, *Electrical efficiency*: *a pore geometric model for the electrical properties of rocks* (Herrick and Kennedy, 1993). Noting that for a class of reservoir rocks whose conductivity depends solely upon the brine they contain (i.e., Archie rocks, see Appendix A), these principles were declared as:

"conductivity σ_t … is a function of the conductivity of the conducting phase (usually brine) σ_w, porosity φ, fractional volume occupied by the conducting phase S_w, and the spatial distribution, or geometry, of the conducting phase. … $\sigma_t = \sigma_w S_w \varphi E$".[6]

Translated into an enumerated list, the declaration has morphed into:

The bulk conductivity of an oil-bearing reservoir rock depends upon:

(1) *brine* conductivity;

(2) fractional volume of *brine* in the rock;

(3) the geometrical configuration of the *brine*.

As you see, the relationship is described in words in terms of unspecified functions, but except for the

---

[5]Pabitra Sen's 1980 article with a section entitled *Derivation of Archie's Law from First Principles* is based upon an effective medium approximation. This hardly meets the definition of a "first principle".

[6] The notation in this quote has been "modernized" to conform to the notation used in this article.

geometrical factor E the formula was written in terms of explicit parameters. For bulk rock conductivity σ_t, the list above was translated into:

   (1) $\sigma_t \propto \sigma_w$;

   (2) $\sigma_t \propto S_w\varphi$;

   (3) $\sigma_t \propto E_t$.

If these are the only dependencies of σ_t then

$$\sigma_t = \sigma_w S_w \varphi E_t \,. \tag{3}$$

An important qualification is that the brine cannot conduct electricity unless the fractional brine volume $S_w\varphi$ has an end-to-end connectivity in a specimen (or the bulk rock). In general, this requires $S_w\varphi$ exceed a minimum value known as a percolation threshold. This qualification is denoted as $\varphi > \varphi_{\vartheta}$ and $S_w > S_{\vartheta}$.

Model Foundations. The meaning of σ_w, S_w, and φ are clear, so it remains only to deduce a form for E_t. The deduction is informed by observations, reason, and the "principle of parsimony", also known as Occam's Razor. It will be convenient to pose the problem in terms of "normalized" conductivity; i.e., instead of considering σ_0 or σ_t, I consider $\sigma_t/\sigma_0 \equiv i$, $\sigma_0/\sigma_w \equiv f$ and $\sigma_t /\sigma_w \equiv g$. (Note that $f = 1/F$ and $g = 1/G$ where F and G are formation resistivity factors as defined by Archie (1942), and Waxman and Smits (1968), respectively.) The first principles are then restated as $g \equiv \sigma_t /\sigma_w$, $g \propto S_w\varphi$, and $g \propto E_t$. Thus $g = S_w\varphi E_t$. I begin the elaboration of E_t by multiplying g by 1 in the form of $1 = E_0 / E_0$ (E_0 to be defined momentarily).

$$g = S_w\varphi E_t \frac{E_0}{E_0} = S_w\varphi \frac{E_t}{E_0} E_0 = S_w\varphi e_t E_0 \,. \tag{4}$$

where $e_t = E_t/E_0$.

Note the grouping of factors on the right side of (4) into the pairs $S_w\varphi$ and $e_t E_0$. S_w is a coefficient quantifying what fraction (i.e., $0 \le S_w \le 1$) of the pore volume φ is brine-filled. Similarly, e_t is a coefficient quantifying the fractional reduction (i.e., $0 \le e_t \le 1$) in the ability of the reduced amount of brine available in the pore volume to contribute to the bulk rock conductivity.

I will now show that E_0 is a function of φ alone, and that e_t is a function of S_w alone. Consider the case where $S_w = 1$. Then $\sigma_t/\sigma_w = \sigma_0/\sigma_w = f$ and $E_t = E_0$; thus $e_t = 1$, and

$$g\big|_{S_w=1} = f = \varphi E_0 \,. \tag{5}$$

Since this relationship holds for g only where S_w is constant and equal to 1, then E_0 must be a function of φ alone. Next consider a case of constant porosity. Then

$$g\big|_{\varphi=constant} = S_w e_t \varphi E_0(\varphi) = S_w e_t \left[\varphi E_0(\varphi)\right] \tag{6}$$

where, since porosity is constant, the factors in square brackets are a constant; so if e_t varies, its variation is a function of S_w alone. Thus $E_t = e_t(S_w)E_0(\varphi)$.

Introducing the conductivity index, $i = \sigma_t / \sigma_0$, will complete the list of definitions needed for the arguments to follow.

Collecting the connections I've made to this point:

$$g = \frac{\sigma_t}{\sigma_w} = \frac{\sigma_t}{\sigma_0}\frac{\sigma_0}{\sigma_w} = i f = \left[S_w e_t(S_w)\right]\left[\varphi E_0(\varphi)\right]. \tag{7}$$

This chain of relationships shows that g can be factored into a product that depends only on water saturation and another factor that depends only on porosity. Comparison of the factors demands that

$$i = S_w e_t(S_w) \quad \text{and} \quad f = \varphi E_0(\varphi) \,. \tag{8}$$

Going forward I will need to use

$$e_t = \frac{i}{S_w} \quad \text{and} \quad E_0 = \frac{f}{\varphi} \,. \tag{9}$$

Above, I have shown that E_0 is a function of φ alone, and that e_t is a function of S_w alone; but what are these functions? There are two avenues to pursue in answering this question. First there is guessing (albeit educated guessing), and second there is observation. The two avenues do intersect, as I shall show.

Parsimony. Up to this point, I have invoked only first principles and deductions from those principles. I now invoke the principle of parsimony and provisionally assert the functions sought are linear in their independent variables (figure 19). That is

$$e_t = a_i S_w + b_i \quad \text{and} \quad E_0 = a_f \varphi + b_f \,, \tag{10}$$

where the suitableness of the functions and the values of the constants a_i, a_f, b_i, and b_f will be determined by inspection of data. The first step in checking the chain of reasoning is to plug the guesses made in (10) into equations (8). The results are

$$i = a_i S_w^2 + b_i S_w \quad \text{and} \quad f = a_f \varphi^2 + b_f \varphi \,. \tag{11}$$

Boundary Conditions. Comparing these proposed relationships to observations, I note that i can vanish at a value of S_w not equal to (and typically greater than) zero (see figures 9-13). Similarly, f can vanish at a value of φ not equal to zero (see figures 17,18).

These boundary conditions for f are quantified as

$$f\big|_{\varphi=1} = \text{(right boundary)} \qquad \frac{\sigma_0}{\sigma_w}\bigg|_{\varphi=1} = 1\ ,$$

$$f\big|_{\varphi=\varphi_g} = \text{(percolation threshold)} \qquad \frac{\sigma_0}{\sigma_w}\bigg|_{\varphi_g \leftarrow \varphi} = 0\ ,$$

and a third condition

Figure 19. The location of two points on the geometrical factor function are known. These are the brine point whose coordinates (1,1) are known, and the percolation threshold whose vertical coordinate is zero, and whose horizontal coordinate is close to the origin. These points are shown as red crosses in (a). The function connecting these coordinates is a priori unknown, but certain functions can be ruled out. For example, an oscillating function (b) is ruled out since a function increasing as volume of the conducting phase increases cannot reverse its trend and decrease again as the volume of the conducting phase continues to increase. The function must therefore be monotone increasing; possible shapes are illustrated in (c). The simplest working hypothesis is that the function is linearly proportional to porosity as shown in (d). Any deviation from linearity would be dictated by observations of trends in particular data sets.

$$f\big|_{\varphi=0} = \text{(left boundary)} \qquad \frac{\sigma_0}{\sigma_w}\bigg|_{\varphi=0} \neq 0\ .$$

It is observed that $\sigma_0/\sigma_w = f \neq 0$ at $\varphi = 0$. This condition cannot be satisfied by $f = a_f\varphi^2 + b_f\varphi$. To satisfy this condition an additional term is required. The function

$$f = a_f\varphi^2 + b_f\varphi + c_f \tag{12}$$

accommodates all of the boundary conditions and is provisionally accepted into the model. Similarly for i;

$$i = a_i S_w^2 + b_i S_w + c_i\ . \tag{13}$$

This requires revisiting equations (10) to replace them with

$$e_i = a_i S_w + b_i + \frac{c_i}{S_w} \quad \text{and} \quad E_0 = a_f\varphi + b_f + \frac{c_f}{\varphi}\ , \tag{14}$$

and revising equations (11) to

$$i = a_i S_w^2 + b_i S_w + c_i \quad \text{and} \quad f = a_f\varphi^2 + b_f\varphi + c_f\ . \tag{15}$$

Erecting the Model. At this point, the derivation is logically complete. Plugging equations (15) into (7) gives the result

$$g = if = \left(a_i S_w^2 + b_i S_w + c_i\right)\left(a_f\varphi^2 + b_f\varphi + c_f\right)\ . \tag{16}$$

I emphasize that so far, equation (16) has been developed from first principles, the principle of parsimony, and boundary conditions. It remains only to compare its consequences and predictions to observations to falsify or validate the model. The necessary comparisons are made by revisiting the pioneers' data as graphed in figures 9-18. These data support the model, and the model could have been deduced empirically by inspection of these data, without reference to first principles. But, using first principles I have dispensed with a priori use of empiricism.

The model itself has more than one useful representation. To illustrate this consider equation (16). You see that g is the product of two quadratic functions. (For what it's worth, mathematicians call this a biquadratic form.) Compare this to the Archie model $g = S_w^n \varphi^m$. Archie's model is certainly more compact. However, note that the Archie model is constrained to contain zero porosity and zero water saturation; i.e., (0,0). Inspection of the pioneers' data figures included in this article will show that none of the data trends include the origin. Likewise, in order to describe some data sets, Archie's model is modified to $g = S_w^n \varphi^m / a$. As you know, the value of a is
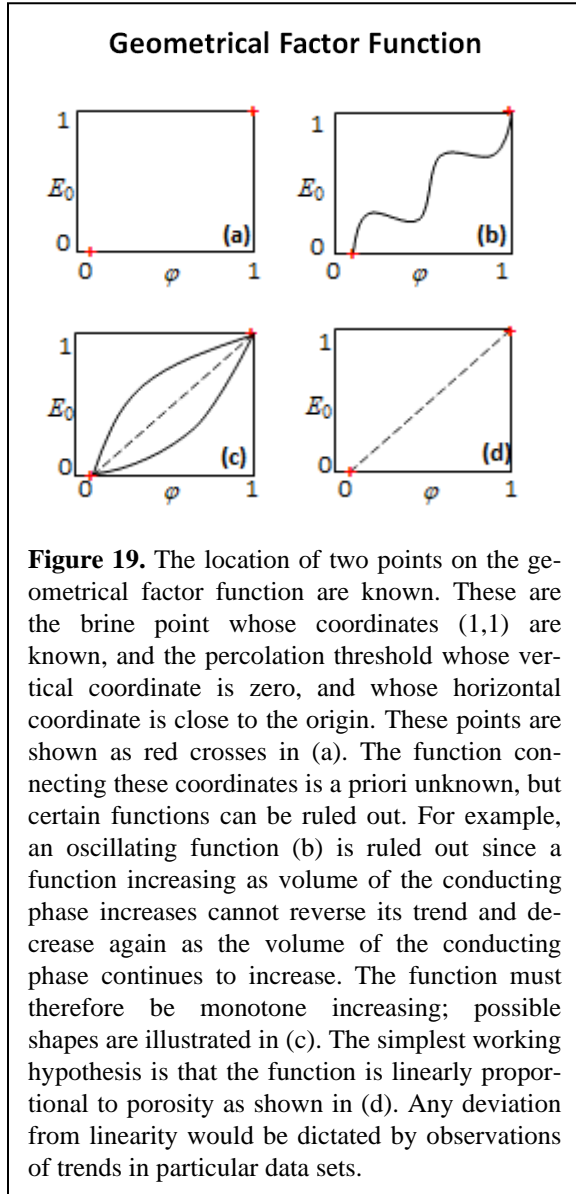
varied to better fit observations, but any value other than $a = 1$ moves the trendline away from one; i.e., $f(1) \neq 1$, which is not a physically realizable condition, and reduces Archie's already empirical model to a mere curve fit, without any physical interpretation.

The representation of quadratic functions as polynomials of second degree is called the "standard" representation. When Excel fits a second-degree polynomial to a set of observed points, it returns its results in this form. This may also be the way you first encountered this conic section in your study of algebra. However, there are other useful representations. For example, the "fundamental theorem of equations[7]" holds that any polynomial of degree n will have n factors. That means a quadratic equation has two factors, and a bi-quadratic form will have four factors. Thus equation (16) can be written as

$$g = i\,f = \left(\frac{S_w - u}{1-u}\right)\left(\frac{S_w - v}{1-v}\right)\left(\frac{\varphi - p}{1-p}\right)\left(\frac{\varphi - q}{1-q}\right). \quad (17)$$

g is the product of i and f, both are quadratics. Therefore i has two roots, u and v; f also has two roots, p and q. The curves are parabolas that contain the points $S_w = 1$, $i = 1$ and $\varphi = 1$, $f = 1$. The zero crossing coordinates of the parabolas are the "roots". I call the model represented in (17) the generalized geometrical factor theory (or model; GGFT); The model has a convenient visual representation as the generalized formation conductivity factor trend surface, discussed below in the **Unit Conductivity Cube** section. .

Equation (17) permits the factorization

$$i = \left(\frac{S_w - u}{1-u}\right)\left(\frac{S_w - v}{1-v}\right) \text{ and } f = \left(\frac{\varphi - p}{1-p}\right)\left(\frac{\varphi - q}{1-q}\right). \quad (18)$$

This gives a view of the two linear factors whose product is the parabola observed in the actual data. I call them the left factor and right factor. Solving for the right factors in terms of the left factors, then

$$\left(\frac{S_w - v}{1-v}\right) = \frac{i}{\left(\dfrac{S_w - u}{1-u}\right)} \text{ and } \left(\frac{\varphi - q}{1-q}\right) = \frac{f}{\left(\dfrac{\varphi - p}{1-p}\right)}. \quad (19)$$

For the cases $u = 0$ and $p = 0$, then

---

[7] You may have learned this as the "fundamental theorem of algebra". I know I did. However, lately the mathematicians have hijacked that name to apply to a more general notion of what an "algebra" is, and have renamed the theorem quoted here as the fundamental theorem of "equations".

$$\left(\frac{S_w - v}{1-v}\right) = \frac{i}{S_w} \text{ and } \left(\frac{\varphi - q}{1-q}\right) = \frac{f}{\varphi}. \quad (20)$$
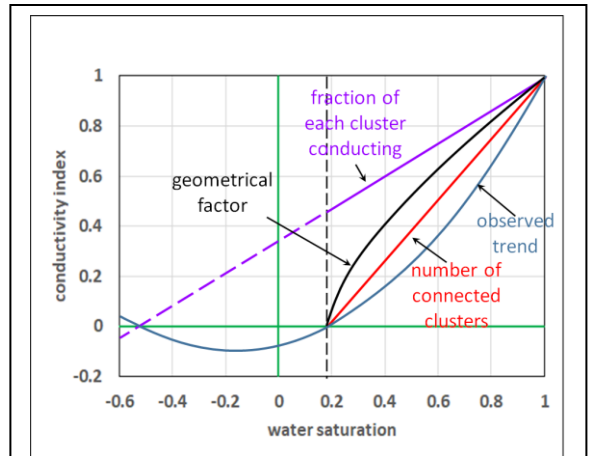
and from (9) you can see that

$$\left(\frac{S_w - v}{1-v}\right) = \frac{i}{S_w} = e_t \text{ and } \left(\frac{\varphi - q}{1-q}\right) = \frac{f}{\varphi} = E_0. \quad (21)$$

Comparing the proposed model of Herrick and Kennedy (1993) in equation (3) to (17), their identity is not immediately obvious.

But, set $u = 0$ and $p = 0$, then

$$\sigma_t = \sigma_w S_w \varphi\left(\frac{S_w - v}{1-v}\right)\left(\frac{\varphi - q}{1-q}\right) = \sigma_w S_w \varphi E_t. \quad (22)$$

Recalling that $E_t = e_t E_0$, equation (3) emerges by letting

Figure 20. The lines in this figure are based upon the trend established by the combined Wyckoff and Botset + Leverett data sets shown in figure 13. The vertical dashed line is the percolation threshold; the "physical" part of the plot is to the right of the dashed line. Percolation theory considers groups of connected pores called "clusters". For lowest porosity, the clusters are disconnected. The boundary between all clusters being disconnected and sufficient connected clusters to conduct end-to-end in a specimen is the percolation threshold. The right factor of the parabola (red line) gives the fraction of connected clusters. Not all the brine in a cluster contributes to conduction. The fraction of brine in each cluster contributing to conduction is represented by the left factor of the trend (purple line). The geometrical factor (or electrical efficiency) is the black line.

$$e_t = \frac{S_w - S_\vartheta}{1 - S_\vartheta} \quad \text{and} \quad E_0 = \frac{\varphi - \varphi_\vartheta}{1 - \varphi_\vartheta}. \tag{23}$$

where I have substituted $S_\vartheta = v$ and $\varphi_\vartheta = q$; these are my notations for percolation thresholds exhibited by i-S_w and f-φ data. Thus, the original geometrical factor model (i.e., 1993) is seen to be a special case of the generalized geometrical factor model.

GRAPHICAL INTERPRETATION OF RESULTS

For the discussion below, refer to figure 20. Formation conductivity factor vs. porosity or conductivity index vs. water saturation data plot as parabolic trends on linear scales. If a trend begins at the brine point and extends below the horizontal axis it will have two roots on the horizontal axis. These three points will determine the shape of a parabola with a vertical axis of symmetry. Since the brine point is not adjustable to fit observations, the two roots determine the parabola's detailed shape. As I have shown, the

parabola can be factored into two lines. Both lines will contain the brine point, and each will contain one of the roots. The line from the brine point through the percolation threshold determines the fractional volume of "connected" brine – that is brine with an end-to-end connection that can carry electric current from one end of a specimen to the opposite end. Above, I called this the right factor. The other line connects the brine point and the left root. The physically meaningful section of this line is to the right of the percolation threshold value. It measures the fraction of the connected brine participating in the conduction. (Some brine will be in stagnant volumes of the pore system, or dead-end pores; this brine does not participate in the conduction of electric current.) Finally, the measure of the "electrical efficiency" of the pore system (that is the ratio of the current flowing in the pore network compared to the maximum current that would flow if the same volume of brine were arranged in an end-to-end tube the same length as the
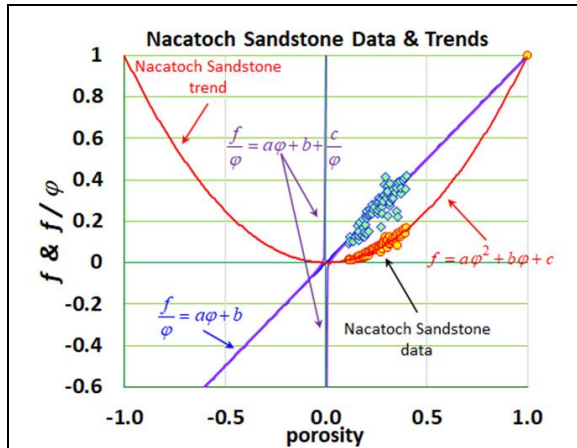
Figure 21.a. Archie's Nacatoch sandstone dataset is atypical in that the trend it exhibits is almost a perfect power law. It is, however, *best* fit by a quadratic. This "zoomed out" figure includes the 73 points in the data set; its zero crossings are invisible at this scale. The trend surface fitting the entire data set is the red curve. The purple function represents this trend line divided by porosity, f/φ. It has two branches and it is discontinuous at $\varphi = 0$. It has the same zeros as the quadratic. However, the trend suggested by plotting f/φ versus porosity is linear since there are no points close enough to the zero to be influenced by its bend toward the horizontal axis. The linear trend through these points is represented by the blue curve.
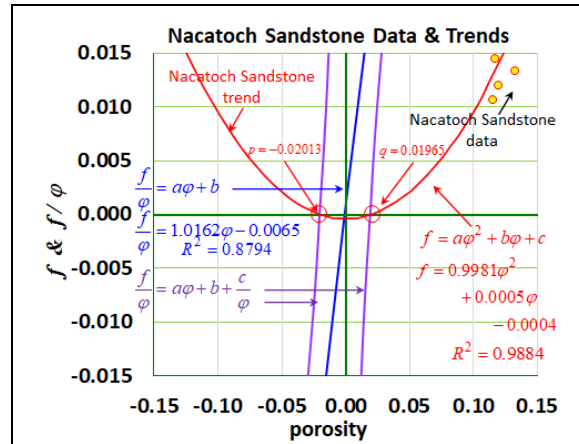
Figure 21.b. The data of figure 21.a "zoomed in" for a closer look at the behavior of the functions near the origin. The zeros of the quadratic are clearly visible; the zeros of f/φ occur at the same points. The blue line is E_f, the same function as f/φ except that the c/φ term is omitted. It appears to intersect the origin, but actually is only close to it. The vertex of the parabola being located at the average value of the zeros, which are not quite equal and opposite. The f/φ function asymptotes to E_0 away from the origin, and curves to asymptote to the vertical (or f) axis at the origin. The "physical" part of the plot is to the right of the right zero. A few of the Nacatoch sandstone data points located at low porosity appear in the graph.

specimen. This is a monotone increasing function of fractional brine volume given by

$$e_t = \frac{i}{S_w} = a_i S_w + b_i + \frac{c_i}{S_w} \text{ and } E_0 = \frac{f}{\varphi} = a_f \varphi + b_f + \frac{c_f}{\varphi}. \quad (24)$$

The roots and the coefficients are related through the quadratic formula. For the formation conductivity factor

$$p, q = \frac{-b_f \mp \sqrt{b_f^2 - 4 a_f c_f}}{2 a_f}, \quad (25)$$

and

$$a_f = \frac{1}{1 - (p+q) + pq}, \quad (26)$$

$$b_f = \frac{-(p+q)}{1 - (p+q) + pq}, \quad (27)$$

and

$$c_f = \frac{pq}{1 - (p+q) + pq}. \quad (28)$$

The roots and coefficients of the conductivity index are similarly related.

Percolation Threshold Model. Observations of data also suggest yet another way to state the second principle:

(2) the rate of change of normalized conductivity with respect to fractional (connected & conducting) brine volume is a linear function of the fractional (connected & conducting) brine volume.

The translation of this principle into a mathematical statement is

$$\frac{df}{d\varphi} \propto \alpha \varphi + b_f \quad (29)$$

where α (alpha) and b are constants to be determined from boundary conditions. Taking the constant of proportionality as one, then
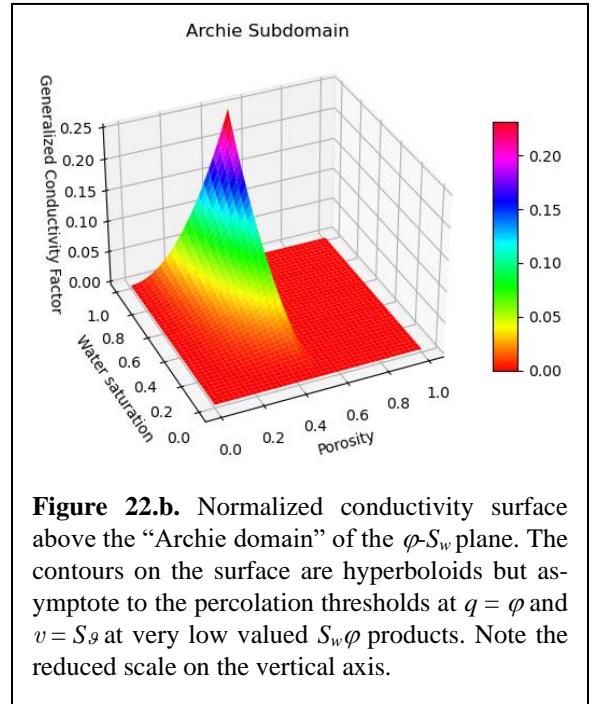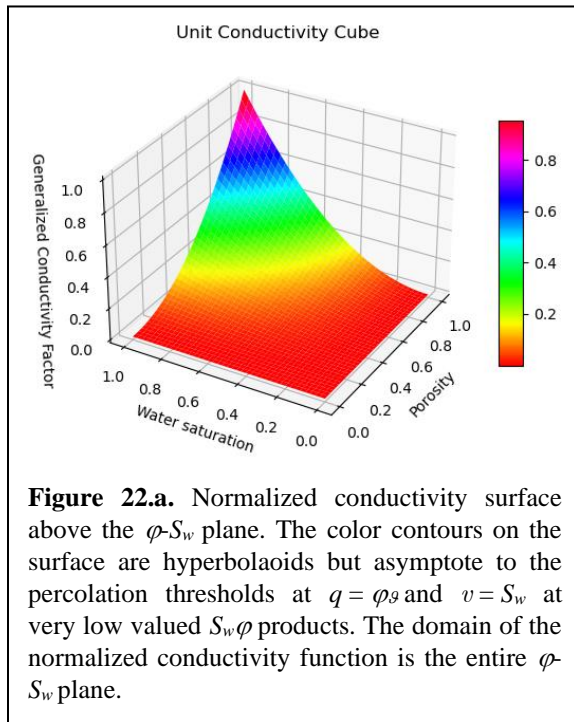
$$\frac{df}{d\varphi} = \alpha \varphi + b_f. \quad (30)$$

Integrating (30)

$$f = \int (\alpha \varphi + b_f) d\varphi = a_f \varphi^2 + b_f \varphi + c_f \quad (31)$$

where $a_f = \alpha/2$. This result is the "standard" form of a quadratic equation, similar to equation (2). Note that implicit in the standard form are the two roots.

The method that Herrick and Kennedy devised for evaluating E_0, which is not directly observable, is to normalize the formation conductivity factor by division by porosity, since both f and φ are directly and routinely observable. Thus, $E_f = f/\varphi$ can be computed for each formation specimen. E_f is then plotted against φ to determine their correlation. In many cases the observed correlation appears to be linear, ex-

Figure 22.a. Normalized conductivity surface above the φ-S_w plane. The color contours on the surface are hyperbolaoids but asymptote to the percolation thresholds at $q = \varphi_\vartheta$ and $v = S_w$ at very low valued $S_w \varphi$ products. The domain of the normalized conductivity function is the entire φ-S_w plane.

Figure 22.b. Normalized conductivity surface above the "Archie domain" of the φ-S_w plane. The contours on the surface are hyperboloids but asymptote to the percolation thresholds at $q = \varphi$ and $v = S_\vartheta$ at very low valued $S_w \varphi$ products. Note the reduced scale on the vertical axis.

pressed as

$$E_f = \frac{f}{\varphi} = a\varphi + b \ . \qquad (32)$$

This is an observation. Note that in the prior publications of Herrick and Kennedy, f/φ is denoted as E_0. I will soon redefine E_0. Equation (32) can be compared with the standard form divided by porosity,

$$\frac{f}{\varphi} = a_f\varphi + b_f + \frac{c_f}{\varphi} \equiv E_0 \ . \qquad (33)$$

where, obviously, the coefficients a_f, b_f, and c_f are unchanged by the division. I have redefined $E_0(\varphi)$ to include the c_f/φ term and to distinguish it from the left factor $E_{f=}(\varphi - p)/(1-p)$. How well does (33) approximate (32)? The difference is in the term c_f/φ. Now c_f is proportional to the pq product which is the product of two small numbers. So, the contribution of this term to the sum is small except as $\varphi \to 0$. Since porosities in conventional reservoirs are usually greater than ten percent, the influence of c_f/φ may be difficult (or maybe impossible) to observe, especially if the data is not "close to" the percolation threshold.

Nonetheless, it is illuminating to take a close look at the f/φ function. To further examine the relationship of data to the f/φ function, I have plotted the function and Archie's Nacatoch sandstone data set in Figure 21.a. Both f and f/φ are plotted. The yellow circles are f values; the blue diamonds are f/φ values.

Figure 21.a shows f/φ as the purple curve over the porosity domain. The function is discontinuous at $\varphi = 0$, as it descends to $-\infty$ to the right of $\varphi = 0$, and descends from $+\infty$ to the left of $\varphi = 0$. The function does have $f/\varphi = a_f\varphi + b_f$ as an asymptote to the left and right of $\varphi = 0$, but begins to deviate markedly from the asymptote near the zeros of the conductivity.

Figure 21.b zooms in on the region of the plot around the origin. This plot makes clear that estimation of the percolation threshold from the linear trend will underestimate the "actual" pseudo-percolation threshold.

DATA AVAILABILITY

Archie had the good luck of having had four data sets available for use in the literature of his time. Since the time of Archie, there is a paucity of data available in the literature. As I have already mentioned, this is a barrier to scholarship. I have already made exten-

sive use of data from Archie and his original sources. I will also use two other published data sets. These are:

Winsauer et al. (1952) published a data set comprising 30 core specimens with extensive measurements on each specimen.

Hamada et al. (2002) published useable formation resistivity factor – porosity and resistivity index – water saturation data for two wells.

Winsauer's Data Set. The Archie Nacatoch sandstone data set is atypical in that, although quadratic, it is not very (or is minimally) "quadratic"; i.e., it is very nearly a pure power law. In order to better illustrate the points to be made for quadratic functions it is convenient to use a more typical-looking data set. Winsauer et al. (1952; figure 18) published extensive data on 30 rock specimens. These data are not ideal for this purpose due to their varied provenances. Nevertheless, the difficulty in obtaining suitable data in the public domain, and the near absence of a percolation threshold in Archie's Nacatoch sandstone data set, prompts me to use Winsauer's data as a surrogate for a typical sandstone to illustrate some fea-
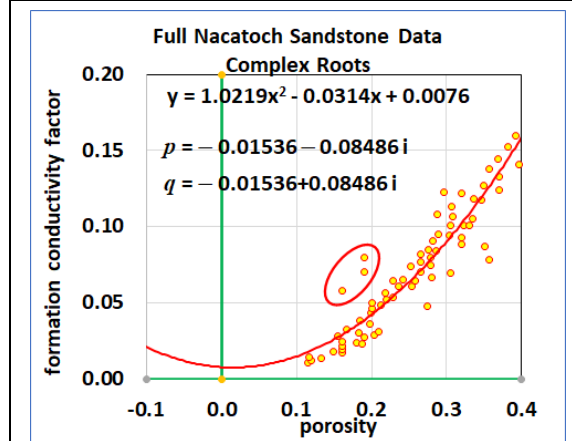
Figure 23. If the trend line does not intersect the porosity axis then its roots are complex conjugate numbers. If the three outliers in the Nacatoch Sandstone data set (northwest of the main trend) are included in the fit, the Nacatoch Sandstone trend will have complex conjugate roots (as shown on the chart above). However, these roots are as effective as real roots for predicting the formation conductivity factor. I have no physical explanation for complex roots other than the data set contains specimens that are unlike the rest of the data, possibly due to fractures or clay.

tures common to most sandstone datasets, and how to analyze those features.

NORMALIZED CONDUCTIVITY AS A SURFACE

Normalization. Formation evaluation relies heavily upon normalized parameters. For example, porosity is void volume of a specimen "normalized" by the bulk volume of the specimen. Water saturation is "bulk volume water" normalized by porosity. Normalization was introduced into log analysis by Archie literally at the very beginning of formation evaluation. Indeed, equation [1] in the Archie paper is $R_0 = FR_w$. The formation resistivity factor F is just the bulk formation resistivity R_0 divided (or "normalized") by the brine resistivity R_w. Whereas R_0 changes whenever R_w or F changes, normalized R_0, that is $R_0 / R_w = F$ is a constant for a given rock specimen. That is to say, F is a property of the rock; if R_w changes, the bulk resistivity will also change in proportion. Note that the range of the normalized resistivity has a lower bound at 1 (that is, R_0 could not be less than R_w), but has no upper bound. This makes the limiting case at high resistivity problematical to represent on a plot. Notice that $1/F$, on the other hand, is bounded between 0 and 1. Moreover, it is related to formation conductivity by $1/F = \sigma_0 / \sigma_w$. The formation conductivity factor is defined as $f = 1/F$, and note that it is bulk formation conductivity normalized by brine conductivity, and is a property of the rock. I have also asserted as "first principles" that the rock conductivity is proportional to porosity and to pore geometry, or $f = \varphi E_0$. This simple relationship immediately suggests that the pore geometry will be the formation conductivity factor normalized by porosity; i.e., $E_0 = f / \varphi$, providing a means to estimate the pore geometric factor. But, does it?

This is not obvious using Archie's formation resistivity factor – porosity power law formula. For example, $1/F = f = \varphi^m$. Where is the pore geometry? The conventional answer is in m; however, by comparison with the GFT model, the pore geometry factor is φ^{m-1}. That is, $f = \varphi \varphi^{m-1} = \varphi E_0$. Normalizing F by φ produces $F/\varphi = 1/\varphi^{m+1}$, which is not useful. The equivalent normalization in the Archie model would be $\varphi F = 1/\varphi^{m-1}$, but in Archie's resistivity formulation, and without guidance from first principles, there is no obvious reason for, or benefit to, doing this. Thus, it was never tried.

The product of resistivity index and formation resistivity factor is $IF = R_t / R_w$. Archie did not give a name

to this quantity, but Waxman and Smits (1968) define it as G. In keeping with this established notation, let

$$\frac{1}{G} = \frac{\sigma_t}{\sigma_w} = i f \equiv g \ . \qquad (34)$$

This is normalized formation conductivity for $S_w < 1$.

The normalized formation conductivity g varies from 0 to 1. Likewise, porosity and water saturation also vary from 0 to 1. Since normalized formation conductivity is a function of both φ and S_w, the representation of g as a surface over the φ-S_w plane suggests itself as a useful way to visualize conductivity-porosity-water saturation data.

The Unit Conductivity Cube. The bulk conductivity of a formation is a function of fractional brine volume, the product $S_w\varphi$. Now, clearly water saturation can vary independently of porosity. Similarly, rock specimens of differing porosity can have the same water saturation; that is, for fixed S_w, porosity can vary. So, although formation conductivity is a function of the $S_w\varphi$ product, the parameters in the product are independent. If the bulk formation conductivity is normalized by brine conductivity, then the inputs, p and q, and the output to $f = ((\varphi - p)(\varphi - q)) / ((1 - p)(1 - q))$ all vary between 0 and 1. The situation is similar for the conductivity index; i.e., $i = ((S_w - u)(S_w - v)) / ((1 - u)(1 - v))$. Then $g = i f$ is also bounded: $0 \leq g \leq 1$.

The normalized conductivity can then be represented as a surface over the S_w-φ plane. The surface is embedded in the volume of a cube with sides of length 1 which I call the "unit conductivity cube". This is a very useful device for visualization and calculation. Figure 22.a illustrates an example of the surface. The domain of the normalized conductivity function is the entire S_w-φ plane. However, since the porosity of rocks does not extend much above 45 percent (if that high) the main interest is in the subdomain with porosity less than 50 percent. I call this the "Archie" subdomain, illustrated in figure 22.b.

As far as the benefit of calculation is concerned, the Archie model dictates the juxtaposition of two separate calculations; one for all of the data at $S_w = 1$ to compute m; the other for each separate specimen to determine an n for that specimen which must then be somehow averaged to produce a single n value to apply to all the specimens. Using the GGFT model all of the adjustable parameters are determined simultaneously, and the need to invent an average for the n values is obviated.

Fractional Volume of Brine. The second principle is expressed in terms of the fractional volume of brine in an Archie rock. The usual notation for this quantity is $S_w\varphi$, "bulk volume water". The domain of water saturation is $0 < S_w \leq 1$; when $S_w = 1$ then the fractional volume of brine is maximized and is numerically equal to the porosity, although they are not the same things. The bulk conductivity of the fluid-filled rock is reduced when conductive brine is displaced by non-conductive hydrocarbon fluids. To characterize this reduction in conductivity, a laboratory procedure is performed where a fully brine-saturated and brine-wet specimen is "drained" by displacing brine using a non-wetting, non-conductive fluid (e.g., air) and the reduction in conductivity is recorded together with the fractional volume of brine remaining in the rock.

Such experiments, as already noted, were the basis of Archie's observation $R_t = R_0/S_w{}^n$. Archie found four such experiments in the literature in the period 1936-1938. The data from Archie's references are illustrated in figure 2 (Archie's figure 3). As I have shown (figures 9-13), a quadratic trend line is strongly suggested. In terms of a formula for the trend, then

$$i = \left(\frac{S_w - u}{1 - u}\right)\left(\frac{S_w - v}{1 - v}\right) \quad (35)$$

where i is the conductivity index and u and v are the roots of the quadratic function.

Equation (17) forms the basis for a saturation equation via

$$g \equiv if = \left(\frac{S_w - u}{1 - u}\right)\left(\frac{S_w - v}{1 - v}\right)\left(\frac{\varphi - p}{1 - p}\right)\left(\frac{\varphi - q}{1 - q}\right) \quad (17)$$
$$\approx S_w^n \varphi^m$$

where I indicate the approximate equality of the Archie model. The formula developed in equation (17) is a generalization of the original geometrical factor theory (Herrick and Kennedy, 1993). Unlike the Archie model, in using the GGFT all of the adjustable parameter values are determined in a single inversion procedure.

Finally, and incidentally, the contours on the normalized conductivity surface are hyperboloids with the pseudo-percolation thresholds as asymptotes. For the case where all of the adjustable parameters are zero:

$$S_w^2 = \frac{g}{\varphi^2}; \quad \Rightarrow \quad S_w = \frac{\sqrt{g}}{\varphi}. \quad (36)$$

For the general case

$$\sqrt{\left[\frac{S_w - v}{1 - v}\right]\left[\frac{S_w - u}{1 - u}\right]} = \sqrt{g} \Big/ \sqrt{\left[\frac{\varphi - p}{1 - p}\right]\left[\frac{\varphi - q}{1 - q}\right]}. \quad (37)$$

SATURATION EQUATION

The function displayed in equation (17) is a biquadratic form with four roots. It is quadratic in both S_w and φ. Solving for terms in S_w gives

$$(S_w - u)(S_w - v) = g\left[\frac{(1-p)(1-q)(1-u)(1-v)}{(\varphi - p)(\varphi - q)}\right]. \quad (38)$$

Once the values for the adjustable parameters are determined, the saturation equation follows from converting to standard quadratic form by expanding the left side and grouping terms, to yield

$$S_w^2 - (u + v)S_w$$
$$+ \left\{uv - \left(\frac{1-p}{\varphi - p}\right)\left(\frac{1-q}{\varphi - q}\right)\left(1 - (u + v) + uv\right)g\right\}, \quad (39)$$
$$= 0$$

or

$$S_w = \frac{1}{2}\left((u + v) \pm \sqrt{(u + v)^2 - 4AC}\right) \quad (40)$$

where

$$AC = uv - \left(\frac{1-p}{\varphi - p}\right)\left(\frac{1-q}{\varphi - q}\right)\left(1 - (u + v) + uv\right)g. \quad (41)$$

Note that u, v, p, and q are all determined from the data set at large and apply to all specimens, while g and φ are for a particular sample. Also note that the terms in the curly braces in (39) are a constant for a given sample, or for a specified depth on a log where $g = \sigma_t / \sigma_w$ and φ are estimated from logging instrument responses. For u, v, p, and q all equal zero, (40) reduces to the Archie model with $m = n = 2$.
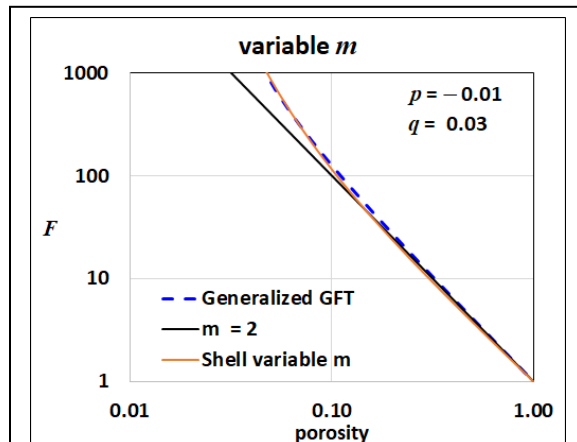
I should say explicitly that reduction to the Archie model in the limit of all of the small parameters becoming zero means that the Archie model is a special case of the GGFT and not the other way around. This explains why when the adjustable parameters of the parabolas diverge slightly from zero, m and n depart from 2 by correspondingly small amounts. The model accounts for the values of m and n being nearly equal since both S_w and φ are quadratic functions (i.e., both S_w and φ appear squared), but also why they are not invariably equal since u and p, and v and q are not constrained to be equal, but are independent parameters.

Complex Roots. Archie's Nacatoch Sandstone specimens have provided much of the evidence used to

make the GGFT model. However, in order to do this it has been necessary to edit out three data points (circled in red in figure 23) which do not appear to be part of the trend as they are more conductive than many other specimens in the same porosity interval. If these data are included and a quadratic fit to them, its roots will be complex numbers. Complex roots do not prevent their use in predicting points on the trend; they are used in the same way real roots are used in equation (17). Due to the paucity of data in the public domain, whether complex roots are due to some physical cause (such as clay), or merely the mixing of incompatible data has not been investigated. A thorough discussion of complex roots is included in Appendix C.

Variable _m_ Model. Schlumberger's 1972 edition of Log Interpretation Charts includes a formula on Chart Por 1 labeled Shell Formula: $m = \varphi^{1.87 + 0.019/\varphi}$ which is called a "variable _m_" formula. The Schlumberger chart book does not include a reference for the formula, so I cannot give attribution to its authors. I will remark that there is no necessity to keep the form of the Archie model; it is simply so ingrained in the thinking of the pioneers at Shell that they felt a need to preserve it. However, this is not a logical requirement. Once the exponent has become a function of porosity, the formula is no longer a power law; any suitable fitting function would have worked as well. In particular, the GGFT provides a means to produce the same trend without any modification of its model, but only a proper choice of its adjustable parameters.

The two models are compared in figures 24. The Shell formula has disappeared from more recent editions of the Schlumberger chart book; however, variable _m_ interpretation remains in use and is a subject of continuing research (Shahi et al., 2018).

Brief Review of PPTT. Probably the first reference to a percolation threshold in a geophysical context was made by Shankland and Waff (1974). They published a formula formally identical to equation (43) below. Their formula was based upon modeling in cubic resistor networks. However, perhaps because they made no connection to petroleum applications, or perhaps because they published in a journal not much consulted by petrophysicists, their contribution had no impact on formation evaluation.
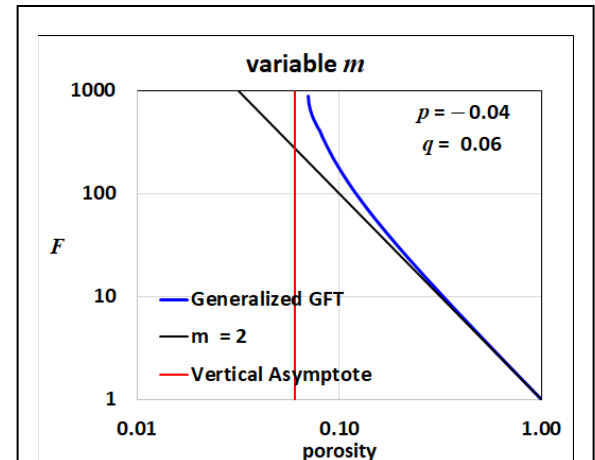
I was ignorant of this prior research as I began my own. Founded upon a careful observation of the Nacatoch sandstone data set, and including the brine point, I speculated (Kennedy, 2007) that

$$\frac{d\left(\sigma_0 / \sigma_w\right)}{d\left(\varphi - \varphi_{\vartheta}\right)} \propto \left(\varphi - \varphi_{\vartheta}\right). \qquad (42)$$

Note that $\varphi - \varphi_{\vartheta}$ is the fractional connected (and conducting) brine volume alluded to in principle 2. Based upon this observation, speculation, and boundary conditions the differential equation implied in (42) is solved to produce

$$\frac{\sigma_0}{\sigma_w} = f = \left(\frac{\varphi - \varphi_{\vartheta}}{1 - \varphi_{\vartheta}}\right)^2. \qquad (43)$$

The complete model, including water saturation was

Figure 24.a. The Shell "variable _m_" $\left(m = \varphi^{1.87 + 0.019/\varphi}\right)$ function is closely duplicated by the Generalized GFT model with roots $p = -0.01$ and $q = 0.03$. The function $F \to \infty$ (i.e., $f \to 0$) rapidly as $\varphi \to 0$.

Figure 24.b. In a resistive formation, such as a tight sand, _F_ bends away from the porosity axis. The function illustrated by the blue curve has roots at $p = -0.04$ and $q = 0.06$. The formation reaches a limit of $f = 0$ ($F = \infty$) at $q = \varphi = 0.06$.
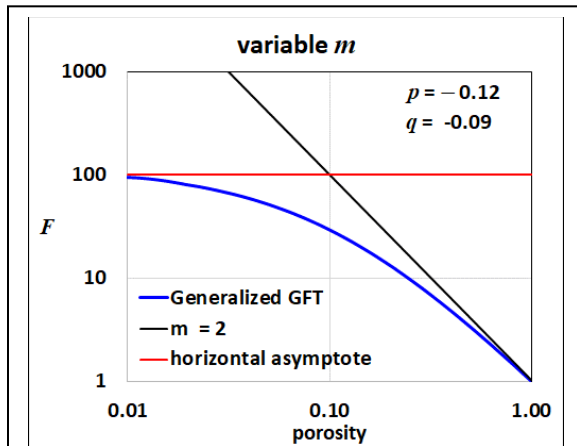
derived as

$$\frac{\sigma_t}{\sigma_w} \equiv g = \left(\frac{S_w\varphi - \vartheta}{1 - \vartheta_l}\right)^2. \qquad (44)$$

where $\vartheta = \mathcal{H}(S_w,\varphi)$ and $\vartheta_l = \mathcal{H}(1,1)$ are generalizations of the percolation threshold on the porosity axis to a contour where g vanishes on the S_w-φ plane. I called this model the pseudo-percolation threshold theory, or PPTT. PPTT turned out to be incomplete because it was based upon an (at the time unrecognized) assumption that the trend parabola was tangent to the porosity axis and touched it only at a single point, the percolation threshold. This is very nearly true for the Nacatoch sandstone (which motivated the PPTT model), but is not generally true. I fixed this deficiency in the 2007 PPTT model by an ad hoc addition to the formula that enabled the parabola to descend below the porosity axis. I did not pursue the consequences of imaginary roots, considering (at the time) such trends to be "unphysical". In hindsight, I was wrong about that.

DEMONSTRATING GGFT

Applied to Hamada et al. Data. Data for illustrating models in the public domain are rare. Hamada (2002) and his coauthors published resistivity-porosity-water saturation data for two wells. The well locations are not disclosed, and the conductivity distributions are disjoint.

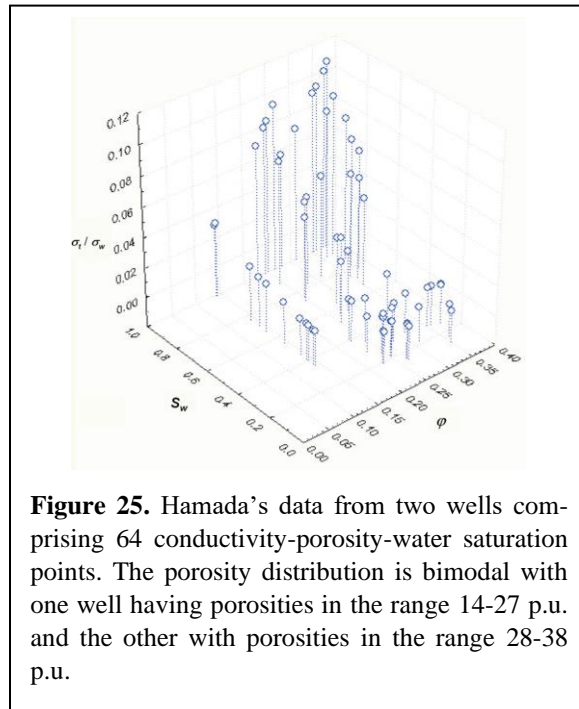However, the porosity intervals covered are closely adjacent on the porosity axis, so the two wells taken together cover a porosity range from 14.2 to 37.4 percent. The resistivity index was sampled at four to six saturation values for each specimen. Taken together there are 64 data triples (illustrated in figure 25), quite enough to characterize a trend surface.

The problem of determining the parameters p, q, u and v is non-linear necessitating a solution by iterative inverse methods such as Newton-Raphson or Levenberg-Marquart. Excel's Solver can also be used if you don't mind "black boxes".

The results are illustrated in figures 26.a through 26.c. The trend surface is qualitatively similar to the surface that would be produced by Archie's model, $g = S_w{}^n\varphi^m$; however, since its parameters are determined simultaneously by the inversion process, it is unnecessary to make a separate computation at $S_w = 1$ to estimate m, or to make any arbitrary decisions regarding how to average n values. Unlike Archie's model which requires the trend surface to contain the origin, the GGFT model relaxes this constraint on power laws and thus can better characterize data trends at low $S_w\varphi$.

LIMITING CASES

Three Special Cases. From equation (17), when $p = u = 0$ the GFT is recovered, and for $p = q$ and $u = v$ the model is reduced to PPTT. Note that for $p = q = u = v = 0$ equations (17) and (40) reduce to the Archie

Figure 24.c. In a conductive formation, such as a shaly sand, F bends toward the porosity axis. The function illustrated by the blue curve has roots at $p = -0.12$ and $q = -0.09$. The formation has a limiting apparent F of 100, or a limiting apparent f of 0.01.

Figure 25. Hamada's data from two wells comprising 64 conductivity-porosity-water saturation points. The porosity distribution is bimodal with one well having porosities in the range 14-27 p.u. and the other with porosities in the range 28-38 p.u.

model formulas with $m = n = 2$. Thus it is seen that (17) is a generalization that includes all of these previous attempts for modeling the conductivity-porosity-water saturation relationship.

EXTENSION TO SHALY SAND

Clay Conduction. Some rocks possess a conduction mechanism in addition to brine. The additional conduction is due to cation exchange on clay crystal surfaces. Since clay is a major constituent of shale, these rocks became known in the well-logging jargon as "shaly sands". Can the geometrical models be extended to shaly sands? The answer is "yes and no", or "it depends".

Waxman-Smits Model. The model of Waxman and Smits (1968, eqn. 22) is

$$C_t = S_w^{n^*} \varphi^{m^*} \left(C_w + BQ_v / S_w \right). \qquad (45)$$

where I adopt the Waxman-Smits notation for conductivity; e.g., $C_w \equiv \sigma_w$, etc. This model is identical to the Archie model except that the brine conductivity is augmented by a contribution from clay surface conductivity. BQ_v is determined on a specimen-by-specimen basis in a laboratory by plotting C_0 against C_w as C_w is varied from 0 to its maximum value (i.e., about 35 S/m for a salt-saturated brine at 75° F). As we have seen, the power laws are approximations of
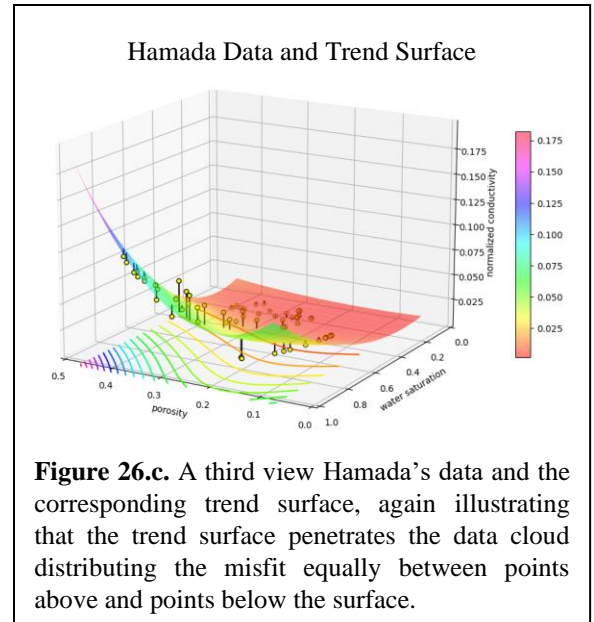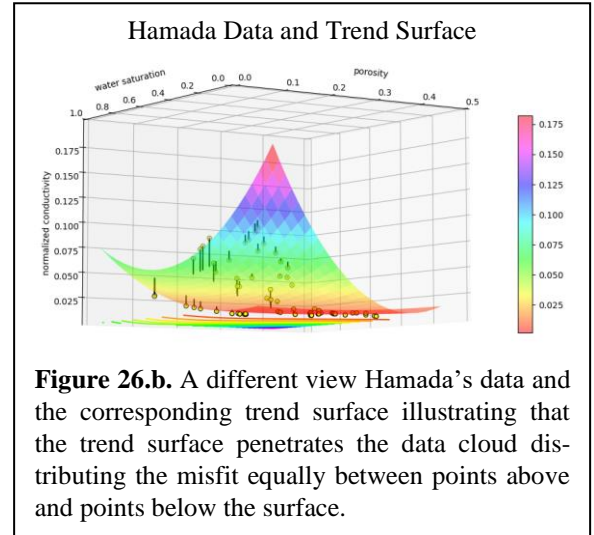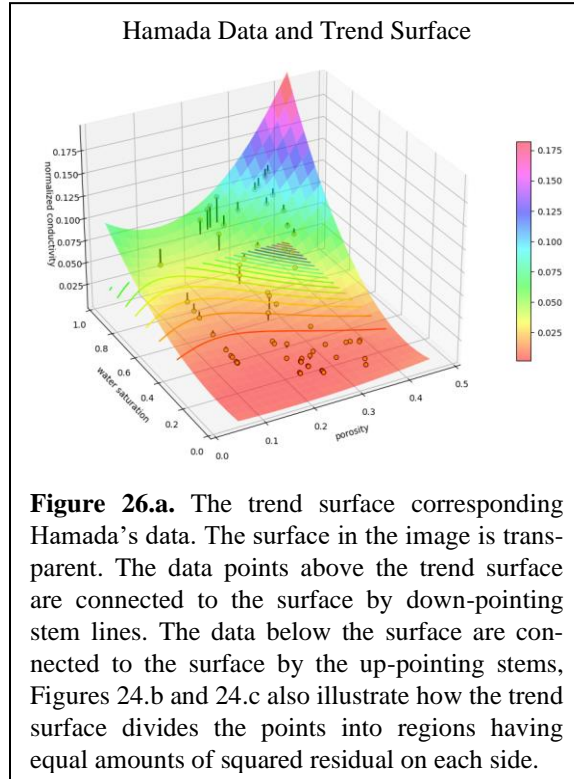
the normalized root form, or

$$S_w^n \varphi^m \approx \frac{C_t}{C_w} = \left(\frac{S_w - u}{1 - u} \right) \left(\frac{S_w - v}{1 - v} \right) \left(\frac{\varphi - p}{1 - p} \right) \left(\frac{\varphi - q}{1 - q} \right). \quad (46)$$

The extension of GGFT to the Waxman-Smits model is a matter of simple substitution. Thus

$$C_t = \left(\frac{S_w - u}{1 - u} \right) \left(\frac{S_w - v}{1 - v} \right) \left(\frac{\varphi - p}{1 - p} \right) \left(\frac{\varphi - q}{1 - q} \right) \left(C_w + \frac{BQ_v}{S_w} \right).$$
$$(47)$$

Since the modification of Archie's model to the Waxman-Smits model is the addition of the BQ_v term to C_w, the efficacy of the model is not changed by the substitution of what amounts to a different fitting, or form, factor.

Figure 26.b. A different view Hamada's data and the corresponding trend surface illustrating that the trend surface penetrates the data cloud distributing the misfit equally between points above and points below the surface.

Figure 26.a. The trend surface corresponding Hamada's data. The surface in the image is transparent. The data points above the trend surface are connected to the surface by down-pointing stem lines. The data below the surface are connected to the surface by the up-pointing stems, Figures 24.b and 24.c also illustrate how the trend surface divides the points into regions having equal amounts of squared residual on each side.

Figure 26.c. A third view Hamada's data and the corresponding trend surface, again illustrating that the trend surface penetrates the data cloud distributing the misfit equally between points above and points below the surface.

Dual Water Model. Compared to the Waxman-Smits model, the dual-water model employs a more physically plausible volume-weighted parallel-conductivity model. However, it is also designed using the Archie model as a template. It is succinctly stated in Clavier, Coates, and Dumanoir (1984, eqn. 1) as

$$C_t = \frac{S_{wT}^n}{F_0} C_{we} = S_{wT}^n \varphi^m C_{we} \qquad (48)$$

where I have supplied the substitution $1/F_0 = \varphi^m$ for clarity. The model differs from the Waxman-Smits model in that the relative contribution to conduction of the brine and clay conducting phases are volume weighted. The weighting of the brine conductivities is modeled as (Clavier et al., 1984, eqn. 4)

$$C_{we} = \left(1 - \frac{v_Q Q_v}{S_{wT}}\right) C_w + \frac{v_Q Q_v}{S_{wT}} C_{cw} \qquad (49)$$

where the *we* subscript is for "effective brine conductivity" and *cw* is for "clay water conductivity". In terms of a parallel conduction model with different geometrical factors for the two conducting phases, the geometrical factor model would be

$$C_t = E_w \left(S_w \varphi - \varphi_{cw}\right) C_w + E_{cw} \varphi_{cw} C_{cw}. \qquad (50)$$

If the geometrical factors happened to be the same, which is the assumption that the dual water model is forced to make, then (50) would become

$$C_t = E_t \left[\left(S_w \varphi - \varphi_{cw}\right) C_w + \varphi_{cw} C_{cw}\right]. \qquad (51)$$

In which case, E_t could be replaced by

$$E_t = S_{wT} \varphi \left(\frac{1 - u/S_{wT}}{1 - u}\right)\left(\frac{1 - v/S_{wT}}{1 - v}\right)\left(\frac{1 - p/\varphi}{1 - p}\right)\left(\frac{1 - q/\varphi}{1 - q}\right). \qquad (52)$$

I make no claims regarding whether GGFT would improve shaly sand interpretations. I only point out that if the model makes the same assumption regarding the geometry of the conducting phases being the same as the Waxman-Smits and Dual Water models do, then GGFT is compatible with these models.

CONCLUDING REMARKS

It has been interesting to return to publications leading up to Archie's discovery of the power law that bears his name. His understanding of the data available to him was grounded entirely in the resistivity formulation of the electrical properties of earth formations, and it is entirely understandable that this should be the case as the resistivity formulation was the basis of electrical and electronic engineering until the introduction of transistors. Moreover, following

the introduction of the Archie model no researcher in the field proposed an alternative view for almost 40 years. The resistivity paradigm was (and is) indeed deeply set.

While the thinking was framed entirely in terms of resistivity, it was impossible not only to answer fundamental questions regarding how rocks conduct electricity, it was impossible even to formulate them for asking. The breakthrough into the realm of the conductivity formulation of this problem began gradually, probably beginning with Waxman's and Smits' 1968 model of the shaly sand problem in terms of conductivity[8]. Their training was in electrochemistry, where the conduction in brines had been formulated in terms of conductivity since early in the development of the science. Even so, their model relied upon translating the Archie model into conductivity terms. This was a breakthrough of sorts, and subsequent shaly sand models were also formulated in conductivity terms.

The 1980s witnessed a shift into considering the problem in terms of conductivity due to the application of the Bruggeman-Hanai model to rocks. This evolution of zeitgeist got doctor David Herrick at Amoco Research rethinking the entire problem of conductivity in petroleum reservoir rocks beginning not with data, but with first principles.

Like much of what is now known about the physical world that was once obscure but now seems obvious, once discovered and explained, the first principles of conduction in rocks now seem obvious: brine does the conducting, therefore (0) the bulk rock conductivity depends on (1) the brine conductivity, (2) the amount of brine available, and (3) the geometry of the brine. Three of these properties are directly accessible to measurement; only the geometry appears to be inaccessible to direct observation. But, it can be estimated from the measurable quantities, and rendered as a function of brine fractional volume by observation and correlation. The resulting model is constructed in the most straightforward manner from these three simple principles. Archie's model falls out of the model as a limiting case.

---

[8] M. R. J. Wyllie introduced a prescient conductivity model in a 1952 conference proceedings article "Clay Technology in Well Log Interpretation." However, he did not pursue this model in his subsequent publications. He also alludes to a preference for conductivity in his 1963 book, *Well Log Interpretation*, 3rd Edition, page 2.

It was eventually realized that the models $\sigma_0 = \varphi^m$ and $\sigma_0 = \varphi E_0$ require σ_0 to vanish together with φ. This is not a property shared by many rocks. The conductivity trend vanishes (or appears to vanish) while the rock retains some brine-filled porosity. Like the Archie model, the geometrical factor theory as originally formulated also implied that conductivity and brine volume should vanish together. With the recognition that conductivity trends in reservoir rocks exhibit percolation thresholds, for the models to work across the entire range of fractional brine volume, percolation thresholds need to be incorporated into any models. Once the need is recognized, it is easily accomplished by modifying the second principle to "the fractional volume of *connected conducting* brine available". The very first formulation of the geometrical factor theory was quadratic in both porosity and water saturation. In general, quadratic functions with a vertical symmetry axis are parabolas in shape and have two roots. In the first edition of the GFT model, the leftmost zero crossing was "pinned" to the origin (i.e., p implicitly assumed to be zero). Once it was realized that a general quadratic function in both porosity and water saturation requires four zeros to attain full generality, the model practically writes itself in terms of the fundamental theorem of algebra, as

$$g = \frac{(S_w - u)}{(1 - u)} \frac{(S_w - v)}{(1 - v)} \frac{(\varphi - p)}{(1 - p)} \frac{(\varphi - q)}{(1 - q)} \qquad (17)$$

where p, q, u, and v are the zeros; two of the zeros (q, v) have physical interpretations as pseudo-percolation thresholds, and the remaining two (p, u) provide two additional adjustable parameters. With special choices for p, q, u, and v, all the models considered in this paper (Archie, GFT, and PPTT) are special cases.

This model has been formulated for an isotropic medium. In general g is anisotropic and is thus a tensor, $\hat{\mathbf{g}}$, so the percolation thresholds will be tensors whenever the formation conductivities are tensors.

The generalized geometrical factor model not only unifies the GFT, PPTT, and Archie models, but also accommodates shaly sand models and niche applications such as variable m models. Since the model follows from obvious physical principles, it provides a theoretical foundation upon which conductivity-porosity-water saturation models can be built and understood. On the other hand, it is only another model; I am reminded of George E. P. Box's admonition: "All models are wrong, but some are useful". The usefulness of petrophysical modeling may ulti-mately vanish along with hydrocarbon exploration and production; in the meantime, let's keep thinking.

This generalization is both illuminating in bringing together several models into the same framework, and useful in that it can be practically applied as an alternative to the Archie model. The model is designed using Archie's original data, so in some parallel universe, Archie himself might have invented it. In our universe, it would be a good thing if some curious researcher with access to a horde of more recent data would validate my results.

In terms of practicality, the data necessary to use the GGFT as an interpretation tool; no new core measurements are required. The workflow would dispense with the independent determination of m and n (and a), using an inversion (or Excel's Solver tool) to determine p, q, u, and v simultaneously in a single procedure. However, at least for well-behaved data, the results are unlikely to be significantly different than the classical Archie-based method. The advantage is that new insights into the rocks may occur, and the intangible satisfaction of knowing there is a solid theory underpinning the GGFT model, of which the classical Archie model is seen to be a special case.

As I close this article, I remind the reader that the generalized geometrical factor theory is derived from first principles. This sets it apart from Archie's purely empirical model. This may open the door to petrophysics reconnecting with the mainstream of geophysics.

I am under no illusion that this article is the last word that can be written on this topic. An example of a recently published model that derives E_0 in terms of tortuosity and constrictivity was published in *Geophysical Prospecting* in December 2021 (Berg et al.). The bridge connecting that new model to this new model parameterized in terms of roots has not begun construction. Bridge builders are needed.

Although every advance in understanding the world will leave some questions unanswered, and perhaps also produce another, deeper level of questions, I am satisfied that the generalized geometrical factor theory unites the various models of conductivity in rocks and provides a framework for future discussion and, perhaps, advancement.

Discussion and criticism of the GGFT model is solicited, encouraged, and welcome.

REFERENCES

Archie, G. E., 1942, The electrical resistivity log as an aid in determining some reservoir characteristics, first issued as T.P. 1422 in Petroleum Technology, and subsequently, *Transactions*, AIME, vol. 146.

Archie, G. E., 1950, Introduction to Petrophysics of Reservoir Rocks: *Bulletin of AAPG*, vol. 39, no. 5, p. 943–961.

Berg, C. F., Kennedy, W. D., Herrick, D. C., 2021, Conductivity in Partially Saturated Porous Media Described by Porosity, Electrolyte Saturation and Saturation Dependent Tortuosity and Constriction Factor, *Geophysical Prospecting*, doi: 10.1111/1365-2478.13166

Bruggeman, D. A. G., 1935, Berechnung verschiedener physikalischer konstanten von heterogenen substantzen: Archiv fur Elektrotechnik, 24, 636–664.

Clavier, C, Coates, G., Dumanior, J., 1984, Theoretical and experimental bases for the dual-water model for interpretation of shaly sands, *SPE Journal* **24**(2), 153-168).

Dwight, H. B., 1961, *Tables of integrals and other mathematical data*: fourth edition, MacMillian Publishing Co., Inc., New York.

Hamada, G. M., Al-Awad, M. N. J., Alsughayer, A. A., 2002, Water saturation computation from laboratory, 3D regression: *Oil & Gas Science and Technology-Rev. IFP*, vol. 57, no. 6, p. 637–651.

Hanai, T., 1968, Electrical properties of emulsions, in P. Sherman, ed., Emulsion Science: Academic Press Inc.

Herrick, D. C. and Kennedy, W. D., 1993, Electrical efficiency: a pore geometric model for the electrical properties of rocks, paper HH, *in* 34th Annual Logging Symposium Transactions: Society of Professional Well Log Analysts.

Herrick, D. C. and Kennedy, W. D., 1994, Electrical efficiency: A pore geometric theory for interpreting the electrical properties of reservoir rocks: *Geophysics*, vol. 59, no. 6, p. 918–927.

Herrick, D. C. and Kennedy, W. D., 1996, Electrical properties of rocks: Effects of secondary porosity, laminations, and thin beds, SPWLA-1996-paper C, *Transactions* of the 37th Annual Logging Symposium: Society of Professional Well Log Analysts.

Jakosky, J. J., Hopper, R. H., 1937, The Effect of Moisture on the Direct Current Resistivities of Oil Sands and Rocks, *Geophysics*., vol. 1, pp. 33-54.

Kennedy, W. D., 2007, The porosity-water saturation-conductivity relationship: An alternative to Archie's model: *Petrophysics*, 48, 335–361.

Kennedy, W. D., Herrick, D. C., 2012, Conductivity Models for Archie Rocks, *Geophysics*, **77**(3), WA109-WA128. DOI: 10.1190/geo2011-0297.1.

Kennedy, D., Garcia, F., 2019, Introduction to Resistivity Principles for Formation Evaluation: A Tutorial Primer, *Petrophysics*, **60**(2), doi: 10.30632/PJV60N2-2019t2

Leverett, M. C., 1938, Flow of Oil-Water Mixtures through Unconsolidated Sands, *Trans*. AIME, pp. 149-171.

Madden, Theodore R., 1976, Random Networks and Mixing Laws, *Geophysics*, Vol. 41, No. 6A.

Martin, M., Murray, G. H., Gillingham, W. J, 1938, Determination of the Potential Productivity of Oil-Bearing Formations by Resistivity Measurements, *Geophysics*, vol. 3, pp. 258-272.

Schlumberger, A. G., 1982, *The Schlumberger Adventure*, Arco Publishing Co.

Sen, P.N.,1981, The dielectric and conductivity response of sedimentary rocks, *Transactions* of 55th Annual Fall Technical Conference and Ex-

hibition of the SPE, Dallas, Texas, Sept. 21-24, SPE 9379.

Shahi, M., Salehi, M. M., Kamari, M., 2018, New correlation for the estimation of cementation factor in Asmari carbonate rock reservoirs, *Egyptian Journal of Petroleum*, Vol. 27, pp. 663-669.

Shankland, T. J., and H. S. Waff, 1974, Conductivity in fluid-bearing rocks: *Journal of Geophysical Research*, 79, 4863–4868, doi: 10.1029/JB079 i032p04863.

Waxman, M. H., and Smits L. J. M., 1968, Electrical Conductivities in Oil-Bearing Sands, SPE *Journal*, **8**(2), 107-122.

Winsauer, W. O., Shearin, H. M., Masson, P. H., Williams, M., 1952, Resistivity of Brine-Saturated Sands in Relation to Pore Geometry, *AAPG Bulletin* 36 (1952): 253-277.

Wyllie, M. R. J., 1952, Clay Technology in Well Log Interpretation, 1st National Conference on Clays and Clay Technology, Berkeley, Calif., July, 1952.

Wyllie, M. R. J., Rose, W. D., 1950, Some Theoretical Considerations Related to the Quantitative Interpretations of the Physical Characteristics of Reservoir Rock from Electric Log Data, *Transactions AIME*, Vol. 189, pp. 105-118, T.P. 2852.

Wyckoff, R. D., Botset, H. G., 1936, The Flow of Gas-Liquid Mixtures Through Unconsolidated Sands, *Physics*, Vol. 7 (September), pp. 325-345.

NOTATION AND GLOSSARY

BQ_v	clay conductivity Waxman-Smits
$C_w, C_0, C_t, C_{cw}, C_{we}$	conductivity dual water
$E, E_a, E_b, E_0, E_{S_w}, E_{cw}$	various geometrical factors
F	formation resistivity factor
FTA	fundamental theorem of algebra
I	resistivity index
S_w, S_{wT}	water saturation
x, y	general algebraic unknown
a, b, c	quadratic form coefficients
cw	dual water subscript for "clay water"
f	$S_w = 1$ formation conductivity factor
g	$S_w < 1$ formation conductivity facto
h, k	coordinates of parabola vertex
i	conductivity index
k	scale factor
m, n	Archie's exponents
p, q, u, v	roots for FTA formulation
$v_Q Q_v$	dual water diffuse layer fraction
ϑ, ϑ_I	percolation threshold contours
α	arbitrary constant
$\varphi, \varphi_{cw}, \varphi_{clay}$	porosities
φ_ϑ	percolation threshold
$\sigma_w, \sigma_0, \sigma_t$	conductivities GFT, GGFT

APPENDIX A. Archie vs. Non-Archie Rocks

Archie Rocks	Non-Archie Rocks
Simple homogeneous pore system only intergranular porosity	**Complex** / heterogeneous pore systems
	Moldic/vuggy porosity Isolated Connected e.g. oomoldic carbonates
	Microporosity discontinuous e.g., microporous chert continuous e.g. authigenic clay coatings
	Laminations or thin beds
	Patchy cement / large grains or clasts
Hydrophilic (brine wet)	**Hydrophobic** (oil wet)
Single conduction mechanism Through intergranular brine	**Multiple** conduction mechanisms Cation exchange on clay minerals Metallic conduction on sulfide minerals e.g. pyrite

Table comparing Archie to Non-Archie rocks. Reproduced from Herrick and Kennedy (1996).

APPENDIX B – Is a Power Law also a Polynomial?

Power Law vs. Polynomial? In conductivity terms, Archie's model is expressed as $f = \varphi^m$ with $m \approx 2$. A true power law would maintain the same slope (that is, the same m exponent) in $\log\varphi$-$\log f$ space over the entire porosity range. The Archie model would also contain the points (0,0) and (1,1). However, the trends defined by many of the various data sets available tend to curve down (for more conductive rocks) or up (for more resistive rocks) in $\log\varphi$ -$\log F$ space and fail to include the points (0,0) and (1,1). A power law in log-log space cannot curve. In general, a second order polynomial would have the form

$$f \equiv \sigma_0/\sigma_w = a\varphi^2 + b\varphi + c \,.$$

When m is identically 2, obviously Archie's model reduces to a second order polynomial with $a = 1$,

$b = 0$, $c = 0$. If a is the dominant coefficient ($a \approx 1$, $b \approx 0$, $c \approx 0$), when plotted on log-log paper, this function will appear to be a power law with $m \approx 2$. How, then, would one decide whether the data underlying the Archie model is one or the other?

Power Law as a Polynomial. The Archie model for rock conductivity posits that $\sigma_0 = \sigma_w \varphi^m$. However, a good case can be made that the relationship observed in the data is equally compatible with a quadratic function, or $\sigma_0 = \sigma_w(a\varphi^2 + b\varphi + c)$. This prompts thoughts on how a power law with non-integer exponent relates to a quadratic, or polynomials in general.

The relationship is investigated by considering the series expansion of

$$f(x) = (1+x)^m. \qquad (B.1)$$

Dwight (1961) provides the series expansion of $f(x)$ as

$$(1+x)^m = 1 + mx + \frac{1}{2!}(m-1)mx^2$$
$$+ \frac{1}{3!}(m-2)(m-1)mx^3 + \cdots \qquad (B.2)$$

The left side is a "power law"; the right side is a polynomial. Consider the substitution

$$\varphi = 1 + x \quad \Rightarrow \quad x = \varphi - 1. \qquad (B.3)$$

Making the substitution

$$\varphi^m = 1 + m(\varphi-1) + \frac{1}{2!}m(m-1)(\varphi-1)^2$$
$$+ \frac{1}{3!}m(m-1)(m-2)(\varphi-1)^3 + \cdots \qquad (B.4)$$

So, we see that φ^m can indeed be represented as a polynomial by the infinite sum. Note that if m is an integer the series vanishes for the $(m+1)^{th}$ and all higher order terms. All the coefficients for terms in the sum less than m will also vanish. The right side is rather complicated. But as an easy to check example for integers, let $m = 2$. Then

$$\varphi^m \big|_{m=2} = 1 + 2(\varphi-1) + \frac{1}{2!}(2-1)2(\varphi-1)^2$$
$$+ \frac{1}{3!}(2-2)(2-1)2(\varphi-1)^3 + 0 + \cdots \qquad (B.5)$$

where I have substituted 2 for m. I have colored the coefficients that evaluate to 1 and 0 red for easy identification. The series truncates at $m = 2$ due to $m - 2 = 0$. The coefficient of the second order term evaluates to 1. Then expanding the parenthesis

$$\varphi^m \big|_{m=2} = 1 + 2(\varphi-1) + (\varphi-1)^2$$
$$= 1 + 2\varphi - 2 + \varphi^2 - 2\varphi + 1 = \varphi^2 \qquad (B.6)$$
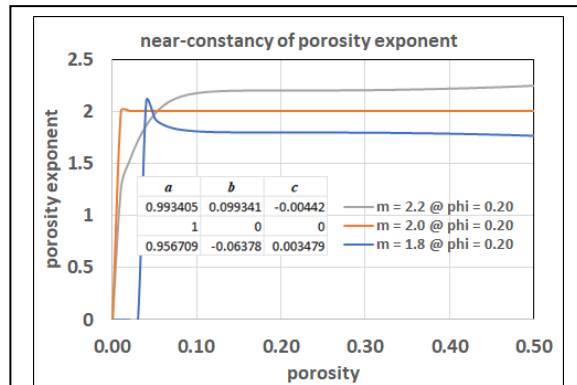
results in the expected identity.

So, for $m = 2$, or any integer, the series truncates. When m is not an integer, the series contains factors of $(\varphi - 1)^p$ with p taking on values 1, 2, 3, and so on. What about higher order terms in these expansions? As an example, we apply the binomial theorem to the cubic term to see that

$$(\varphi-1)^3 = \varphi^3 + 3\varphi^2 + 3\varphi + 1. \qquad (B.7)$$

Obviously, each higher order term (i.e., $p > 2$) has all of the lower order terms represented in its expansion, so the coefficients of the powers of φ on the right side of (B.4) must themselves be expressed as infinite sums. Thus, a power law does have a representation as a polynomial, albeit an infinite one. For integer exponents in power laws, the power-law expands to a one-term series identical to the power law.

$$\varphi^m = \left[\frac{1}{0!}\right](\varphi-1)^0 + \left[\frac{m}{1!}\right](\varphi-1)^1 + \left[\frac{1}{2!}m(m-1)\right](\varphi-1)^2$$
$$+ \left[\frac{1}{3!}m(m-1)(m-2)\right](\varphi-1)^3 + \cdots \qquad (B.8)$$

From the series expansion above it is apparent that the coefficients of the power series on the right side of (B.8) are functions of m, when all of the binomial factors ($\varphi - 1$)^p ($p = 1, 2, 3, ...$) are expanded and their terms collected according to powers of φ, are also functions of φ. To evaluate them begin by find-

	a	b	c	
	0.993405	0.099341	-0.00442	m = 2.2 @ phi = 0.20
	1	0	0	m = 2.0 @ phi = 0.20
	0.956709	-0.06378	0.003479	m = 1.8 @ phi = 0.20

Figure B.1. These curves are generated from quadratic functions with coefficients computed from equations (B.9) - (B.11) at $\varphi = 0.20$ for three different m values. The quadratic functions are then extended over the porosity domain $0 \le \varphi \le 0.40$. Note that m is nearly constant for porosities > 0.10, but unstable at low porosities. This suggests that one reason that the Archie model sometimes fails are low porosity, requiring a change to variable m models.

ing $a_0(m)$ for the special case $\varphi^m \approx a\varphi^2 + b\varphi + c$. Differentiating twice then

$$a(m,\varphi) = \frac{1}{2}(m-1)m\varphi^{m-2}. \qquad (B.9)$$

Using the intermediate results of the differentiations and some algebra gives

$$b_0(m,\varphi) = m\varphi^{m-1}(2-m), \qquad (B.10)$$

$$c_0(m,\varphi) = \frac{\varphi^m}{2}(m^2 - 3m + 2). \qquad (B.11)$$

Substitution of $m = 2$ will produce $a_0 = 1$, $b_0 = 0$ and $c_0 = 0$. These coefficients are the same as those computed using the infinite series; however, the three-term series for φ^m is an approximation (except for integer m) since the higher order terms do not appear because of the special case assumed at the beginning.

Is $ax^2 + bx + c$ a Power Law? The expression

$$\varphi^m \approx a_0\varphi^2 + b_0\varphi + c_0 \qquad (B.12)$$

allows an answer. Taking logarithm of (B.12) and solving for m,

$$m = \frac{\log\left(a_0\varphi^2 + b_0\varphi + c_0\right)}{\log \varphi}. \qquad (B.13)$$

So the quadratic is equivalent to the power law when a solution to (B.13) is possible. Note that for the GGFT model c_0 is constrained to be $c_0 = 1 - (a_0 + b_0)$, but a_0 and b_0 are constrained only by the condition that they describe a parabola with a vertical axis of symmetry. Thus, m will be a decimal fraction except in special cases. As a check, note that

$$m = \left.\frac{\log\left(a_0\varphi^2 + b_0\varphi + c_0\right)}{\log \varphi}\right|_{\substack{b_0=0 \\ c_0=0}} = \frac{\log\left(a\varphi^2\right)}{\log \varphi}$$

$$= \left.\frac{\log(a) + 2\log(\varphi)}{\log \varphi}\right|_{a_0=1} = 2 \qquad (B.14)$$

for the special case $a_0 = 1$, $b_0 = c_0 = 0$.

The bottom line is that every power law has a representation as a power series, truncated or infinite, but not every quadratic function is a power law.

APPENDIX C. Complex Roots

The parabola with a vertical axis of symmetry can be parameterized in a number of ways. The most familiar is the "standard" form

$$f \equiv \sigma_0/\sigma_w = a\varphi^2 + b\varphi + c. \qquad (C.1)$$

In this form the roots are found using the familiar "quadratic formula". However, the same parabola can be parameterized in terms of its vertex (h,k), viz.

$$\frac{y-k}{1-k} = \left(\frac{x-h}{1-h}\right)^2. \qquad (C.2)$$

Solved for y

$$y = k + (1-k)\left(\frac{x-h}{1-h}\right)^2. \qquad (C.3)$$

Lastly, in fundamental theorem of algebra terms, y is written in terms of its factors, or roots, as

$$y = \left(\frac{x-p}{1-p}\right)\left(\frac{x-q}{1-q}\right). \qquad (C.4)$$

Note that whereas a, b, and c, also k and h, are real numbers for any parabola with vertical axis of symmetry, p and q will be complex numbers if the vertex of the parabola is above the x axis. However, any of these parameter sets can be related to all of the others. With these relationships known, the trend surface of a data set can be determined in terms of the parameters a, b, and c, or k and h, and the roots p and q or p and p^* determined from the transforms. In terms of the vertex parameters using

$$p = h - (h-1)\sqrt{-k/(1-k)} \qquad (C.5)$$

and

$$q = h + (h-1)\sqrt{-k/(1-k)}. \qquad (C.6)$$

When the y coordinate of the vertex (i.e., k) is positive, then p is complex and $q = p^*$.

In terms of the coefficients of the standard equation, the formula is

$$p,q = \frac{-b \mp \sqrt{b^2 - 4ac}}{2a} \qquad (C.7)$$

Thus, it is unnecessary to explicitly construct a trend in terms of its complex conjugate factors; two alternatives using only real numbers are available.
The inverse transforms are

$$h = \frac{1}{2}(p+q) \qquad (C.8)$$

and

$$k = \frac{pq - (p+q)^2/4}{1-(p+q)+pq}, \qquad (C.9)$$

Since spreadsheet programs (e.g., Excel) often have a polynomial curve-fitting function in terms of the coefficients of the standard form, in terms of these coefficients the vertex coordinates are

$$h = -\frac{b}{2a} \qquad (C.10)$$

and

$$k = \frac{b^2/4a^2}{2b/4a - 1}. \qquad (C.11)$$

To complete the set of transforms, the coefficients in terms of the vertex and the roots are

$$a = \frac{1}{1-(p+q)+pq} = \frac{1-k}{(1-h)^2}, \qquad (C.12)$$

$$b = \frac{-(p+q)}{1-(p+q)+pq} = -2\frac{1-k}{(1-h)^2}h, \qquad (C.13)$$

and

$$c = \frac{pq}{1-(p+q)+pq} = \frac{1-k}{(1-h)^2}h^2 + k. \qquad (C.14)$$

These results are developed for the case of $y = f$ and $x = \varphi$ in (C.4). Analogous results hold when $y = i$ and $x = S_w$ in (C.4). In that case the parameters p and q are replaced by u and v and the vertex coordinates are denoted s and t.